Applications of XAFS to materials and nano – science

Federico Boscherini

Department of Physics and Astronomy

University of Bologna, Italy

federico.boscherini@unibo.it

www.unibo.it/faculty/federico.boscherini

Plan

- Introduction
  - Review basics of XAFS
  - Characteristics of the technique
  - Role of XAFS
- Examples of applications, using both
  - results which have "stood the test of time"
    - Why? Because we tend to **forget** work done by others some time ago (or don't bother searching the literature) and **do the measurements again**!
      - It will get published in the end, but **not a good use of time & money**!
  - recent results

X-Ray Absorption Fine Structure

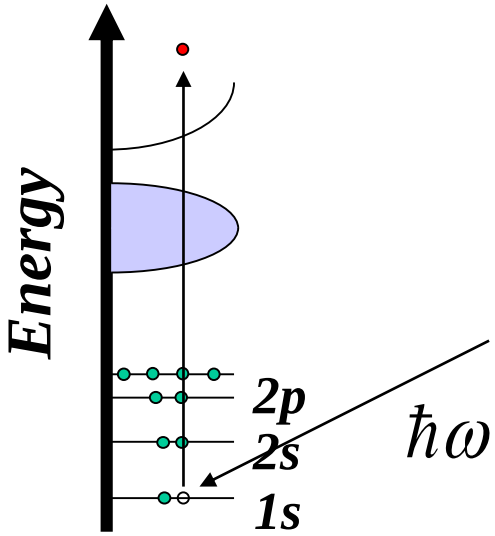

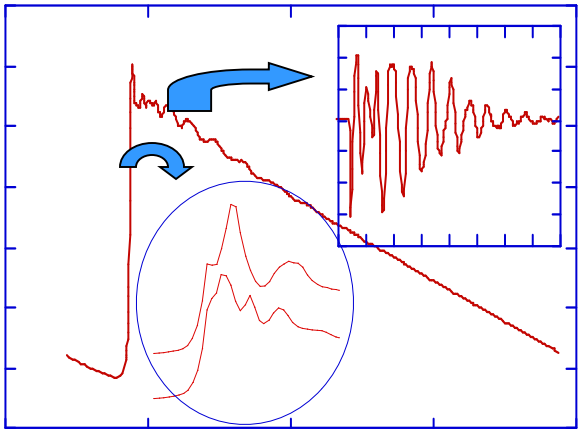

ħω

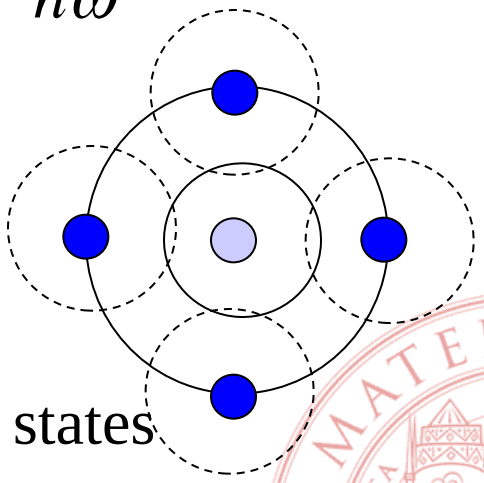

- "EXAFS": Coordination numbers
  Interatomic distances
  Disorder of distances

- "XANES": Absorber symmetry and
  valence/oxidation state
  Electronic structure of unoccupied states
  Medium range structure

EXAFS

- Extended X-ray Absorption Fine Structure
- When applicable, fit with the "standard" EXAFS equation

From *ab-initio* calculations or from reference compounds

$$\chi(k) = S_0^2 \sum_{j=shells} N_j A_j(k) Sin[2kr_j + \overbrace{\varphi_j + 2\delta_1}] e^{-2k^2\sigma_j^2}$$

$$k = \frac{\sqrt{2m(\hbar\omega - E_B)}}{\hbar}$$

Measure:

- Coordination number
- Interatomic distance
- Debye Waller factor
  - thermal vibration
  - static disorder

XANES

- X-ray Absorption Near Edge Structure (also NEXAFS)

$$\sigma(\hbar\omega) = 4\pi^2 \alpha \hbar\omega \left| \langle i | \hat{\varepsilon} \bullet \vec{r} | f \rangle \right|^2 \rho(E_f)$$

$$\Delta\ell = \pm 1, \ \Delta m_\ell = 0$$

(lin. pol. light)

- "Molecular orbital" approach: 1 electron approximation, constant matrix element: probe site and symmetry projected density of states of final electronic states
- "Multiple scattering" approach: structural interpretation through simulation

Characteristics of XAFS

- Atomic selectivity (choose Z via photon energy)
- Equally applicable to ordered or disordered matter
- A core level technique: a local probe
- Interesting underlying physics
- Sensitive to high dilutions
- EXAFS: high distance resolution
- XANES: 3D structural sensitivity
- Recent developments:
  - Sub μm spot size
  - ns, ps and …fs time resolution
  - **Combined use of XES / RIXS**

Role of XAFS in Materials Science

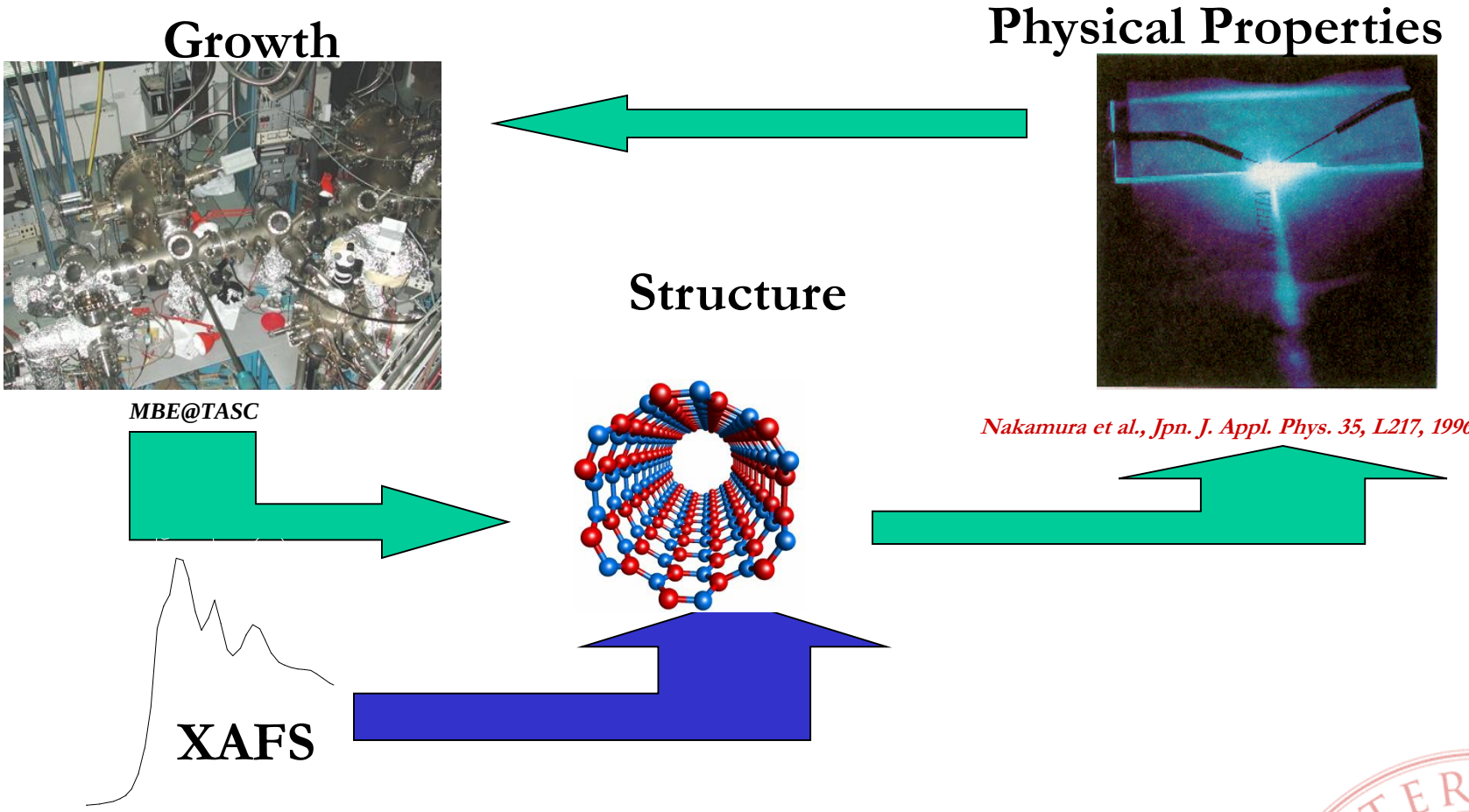

***Objective**: an understanding of physical properties of novel materials based on knowledge of their local structure*

Today's topics

- Dopants, defects
- Alloys
- Phase transitions
- Thin films, interfaces, surfaces
- Nanostructures
  - Semiconductor dots
  - Metallic clusters

XAFS and dopants/dilute elements

- Only the structure around the photo-excited atom is probed
- Fluorescence detection greatly enhances sensitivity
- Present sensitivity limit (depends on sample)
  - dopants in the bulk
    - EXAFS ~ 10^{18} at/cm^3
    - XANES ~ 10^{17} at/cm^3
  - thin films (single layer) ~ 10^{14} at/cm^2

Si in GaAs

S. Schuppler, D.L. Adler, L.N. Pfeiffer, K.W. West, E.E. Chaban, and P.H. Citrin, Appl. Phys. Lett. **63**, 2357 (1993) and Phys. Rev. B **51**, 10527 (1995)

- Si common dopant in GaAs
- Si:GaAs exhibits deactivation
- Accepted explanation : amphoteric nature of Si
  - Si_{Ga} (Si in Ga site): donor
  - Si_{As}: acceptor
  - At low concentration all Si_{Ga}, at higher concentrations both: autocompensation

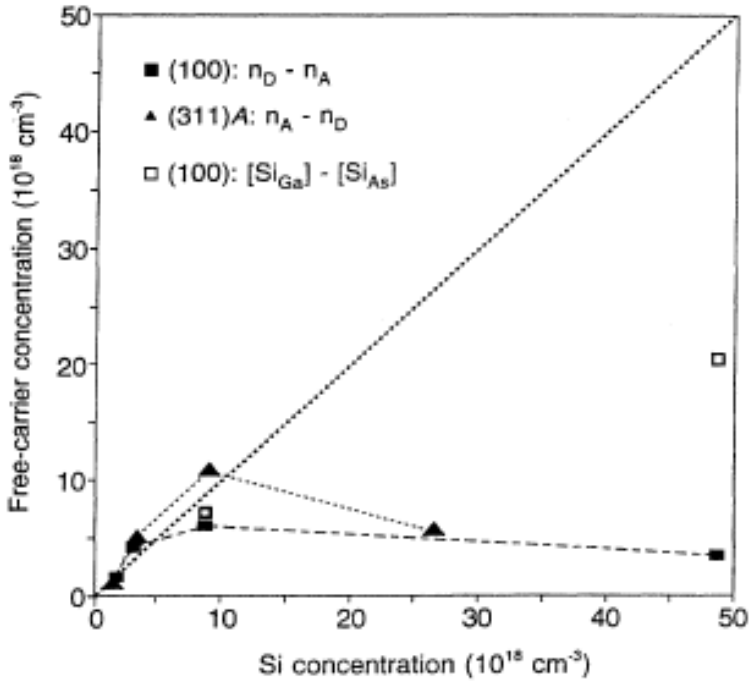

Si in GaAs: XANES

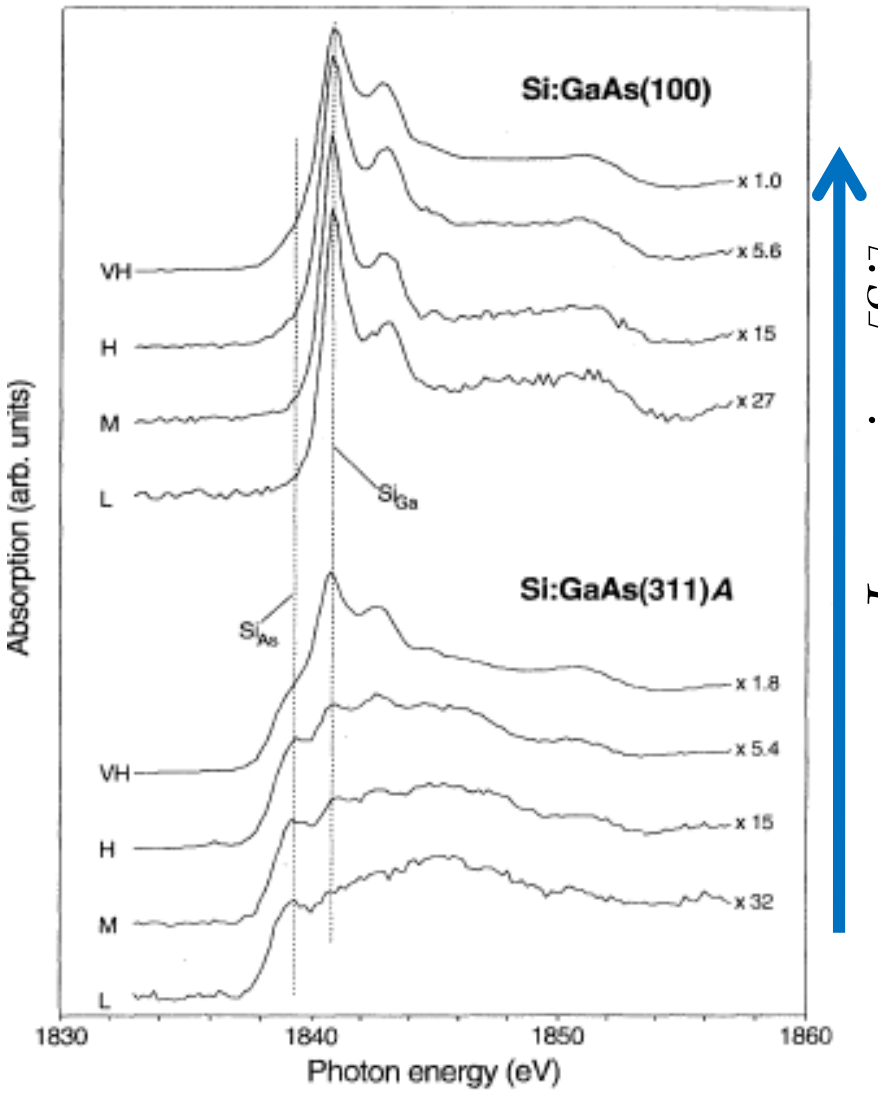

- Samples studied
  - Si:GaAs(001)
    - at low concentration Si_{Ga}
  - Si:GaAs(311)A
    - at low concentration Si_{As}
- XANES exhibit reasonable evolution with concentration
- Difference in lineshape between Si_{Ga} and Si_{As} due to difference in charge on Si and conduction band DOS

Si in GaAs: XANES

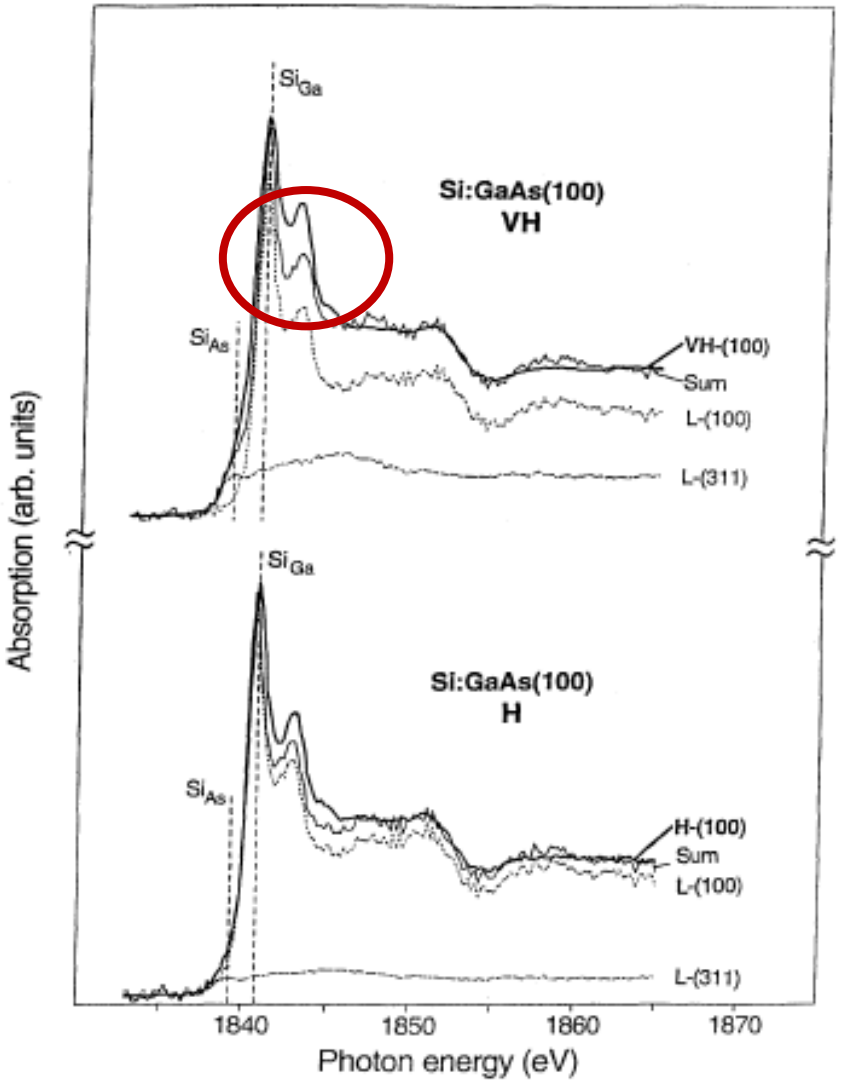

- Fitting of Very High concentration sample indicated that lineshape cannot be explained only on the basis of combination of Si_{Ga} and Si_{As}

Si in GaAs : EXAFS

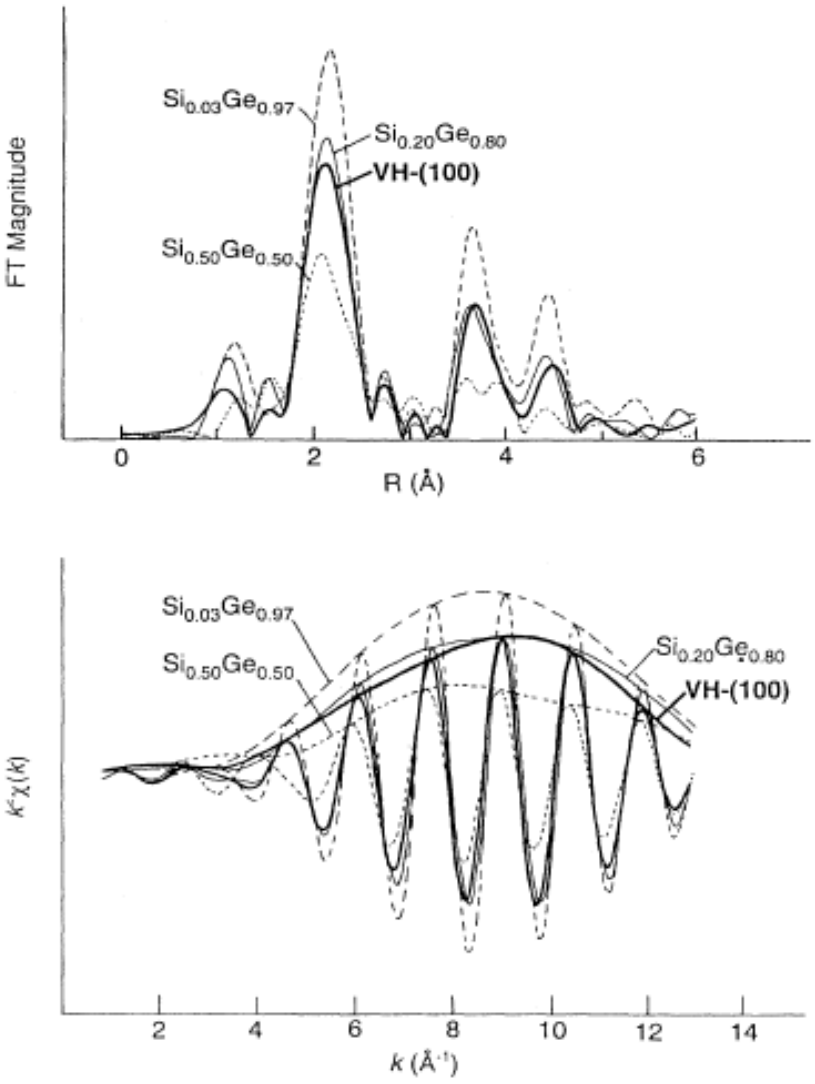

- Compare EXAFS spectra with those of Si_xGe_{1-x} random alloys
- Ge has similar scattering amplitude to Ga and As
- VH sample spectrum very similar to $Si_{0.2}Ge_{0.8}$
  - 20% of Si is bonded to Si
- Conclusion: deactivation due also to presence of **Si dimers and clusters**

Fe in GaN

•A. Bonanni, A. Navarro-Quezada, Tian Li, M. Wegscheider, Z. Matěj, V. Holý, R. T. Lechner, G. Bauer, M. Rovezzi, F. D'Acapito, M. Kiecana, M. Sawicki, and T. Dietl, Phys. Rev. Lett. **101**, 135502 (2008)
• M. Rovezzi, F. D'Acapito, A. Navarro-Quezada, B. Faina, T. Li, A. Bonanni, F. Filippone, A. Amore Bonapasta, and T. Dietl, Phys. Rev. B 79, 195209 (2009)
• A. Navarro-Quezada, W. Stefanowicz, Tian Li, B. Faina, M. Rovezzi, R. T. Lechner, T. Devillers, F. D'Acapito, G. Bauer, M. Kiecana, M. Sawicki, T. Dietl, and A. Bonanni Phys. Rev. 81, 205206 (2010)

- Candidate material for spintronic applications
- Grown by Metal Organic Vapor Phase Epitaxy
- Fe concentrations
  4×10^{19} cm^{-3} - 4×10^{20} cm^{-3}
- Aims:
  - Determine the site of Fe in GaN
    - Determine the effect of Si co-dopant
    - Correlate with magnetic properties

Fe:GaN data

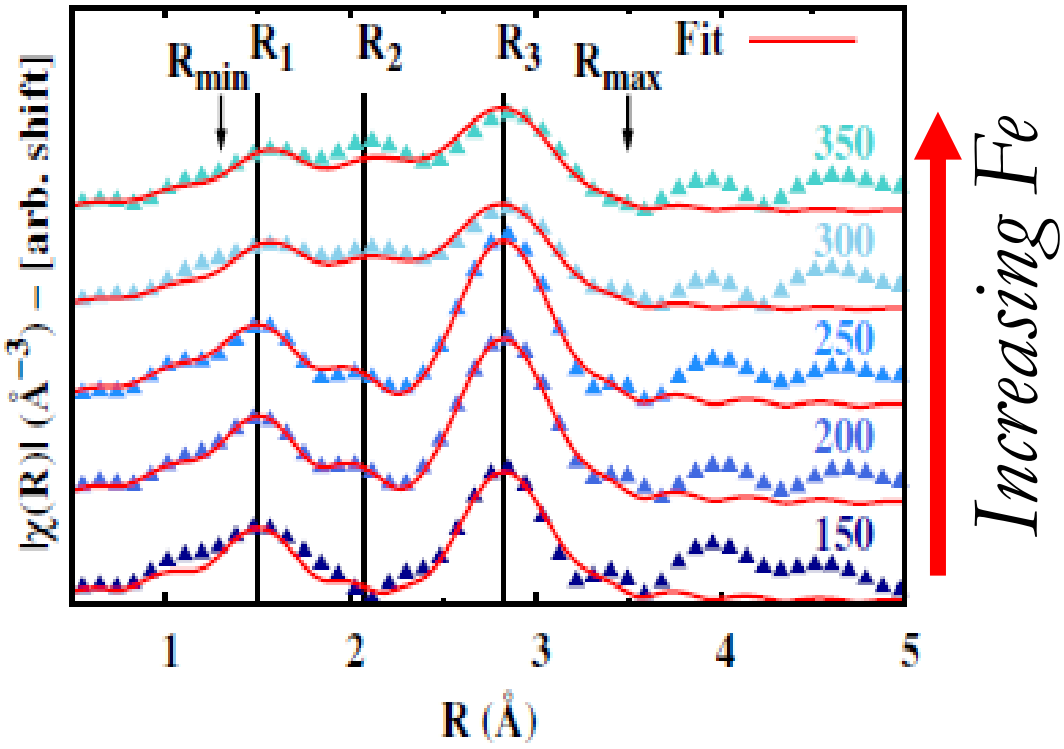

Low Fe content:

- only two Fe-N (R_1) and Fe-Ga (R_3) bonds.
- Fe substitutional; bond length in agreement with DFT for Fe^{3+}

High Fe content

- Appearance of Fe-Fe (R_2) coming from a precipitated Fe_xN phase

Si,Fe:GaN data

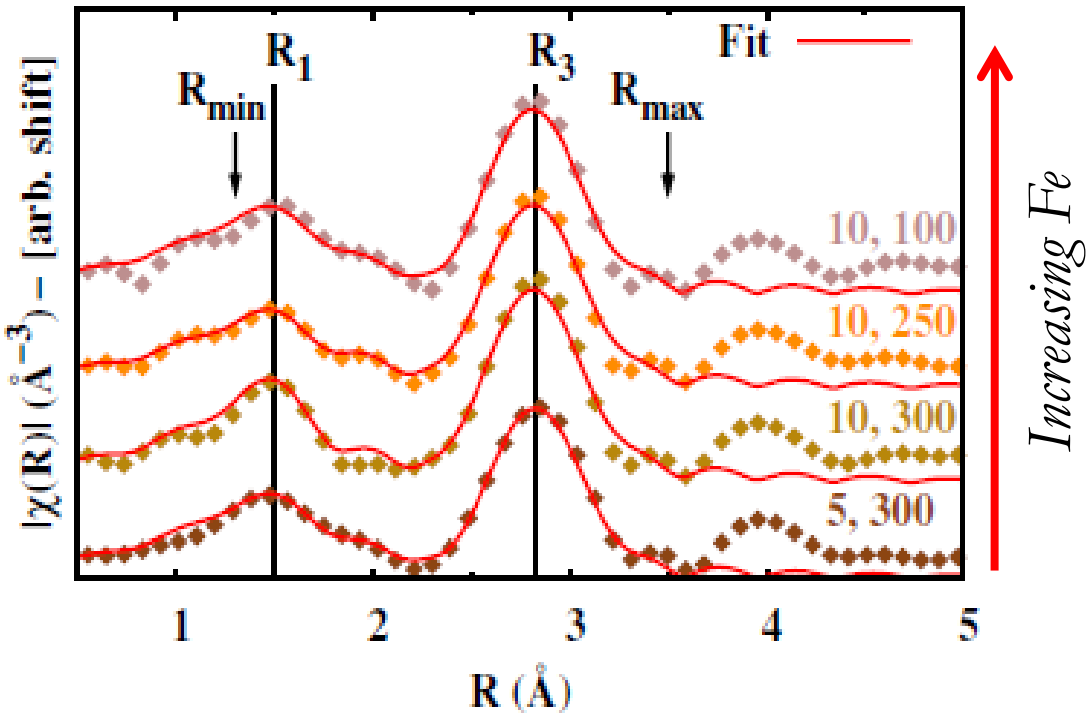

- For the same Fe content Si co-doping prevents the formation of Fe_3N
- No evidence of the Fe-Fe bond at R_2

Si affects the charge state of Fe

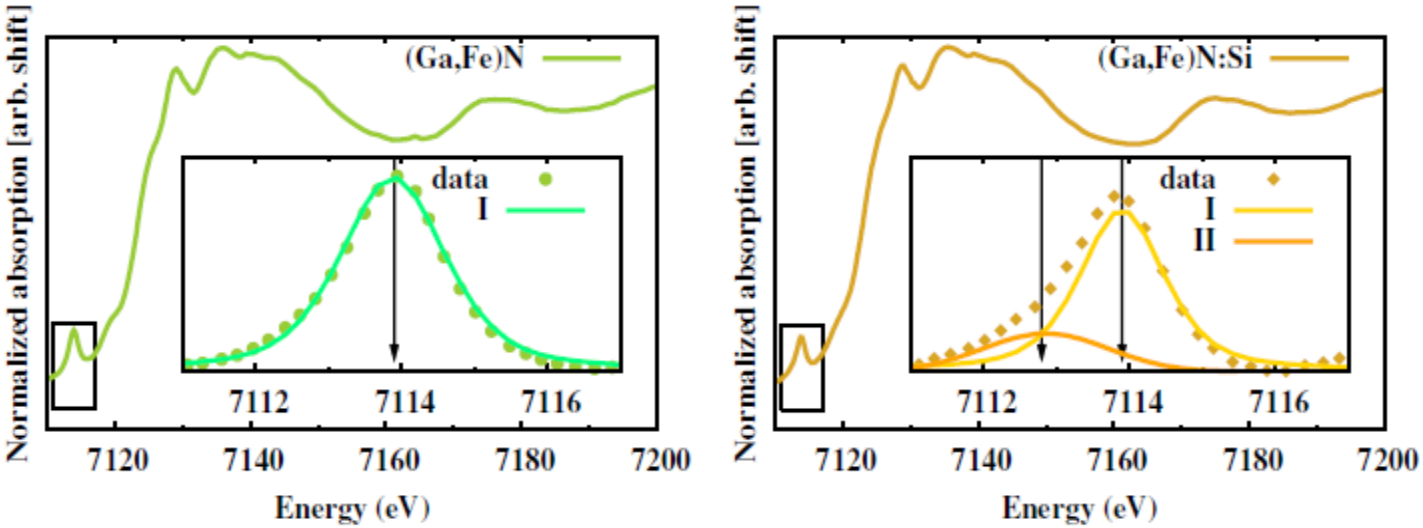

- Si addition causes partial reduction of Fe^{3+} ions to Fe^{2+}
- Notable ability of XAFS to determine structure and valence

Role of the growth temperature

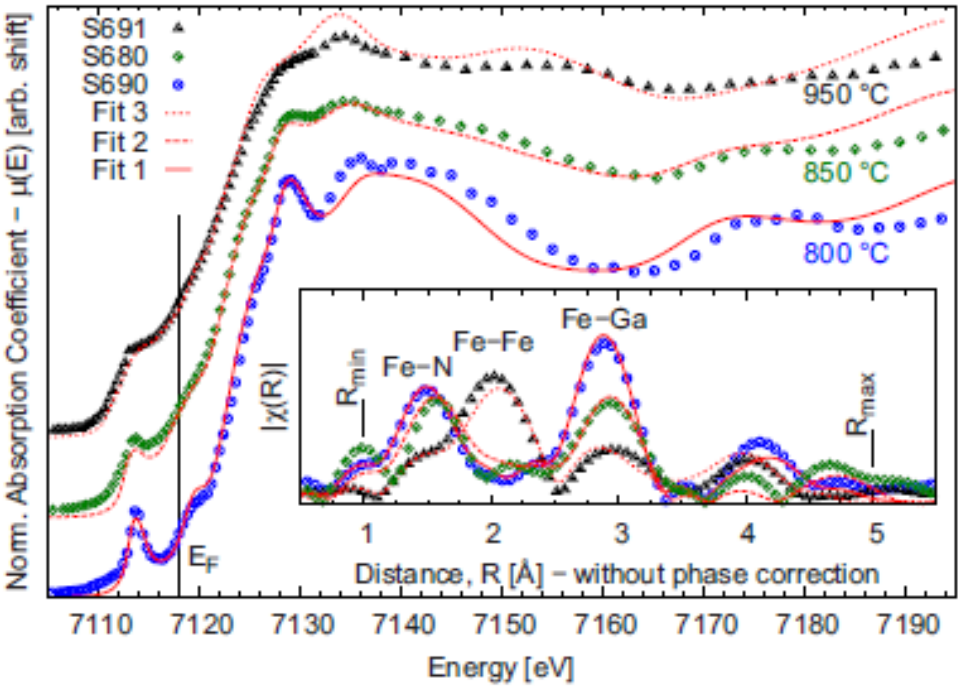

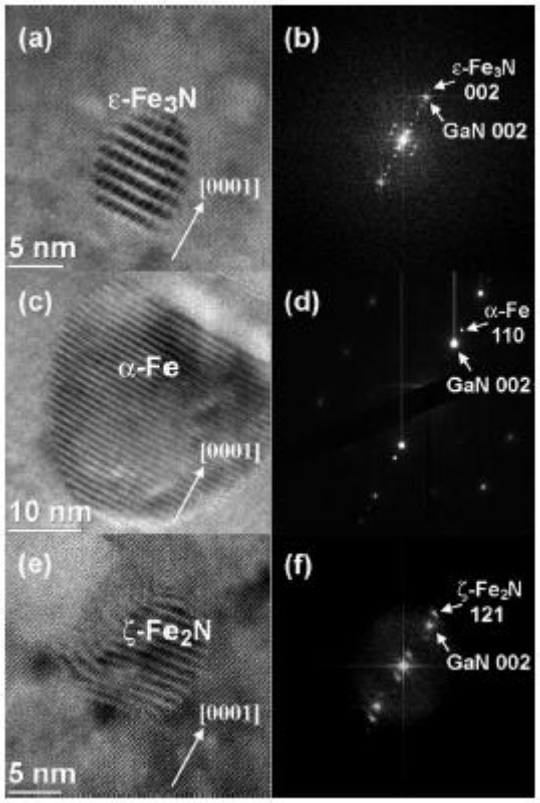

- Higher growth temperature favours formation of Fe_xN and α-Fe

Fe:GaN conclusions (2010 paper)

- Magnetization due to various components, including one due to ferromagnetic nanocrystals of ε-Fe_3N, α-Fe, γ'-Fe_4N, γ-Fe_2N and γ-Fe
- Si codoping reduces the formation of Fe rich nanocrystals and permits a higher incorporation of Fe.
- Use new term: (Ga,Fe)N nanocomposites, not real doping

Metal precipitates in Si solar cells

Buonassisi et al, Nature Mat. 4, 676 (2005)

- Supply of high purity Si << demand
- Use of lower purity material
- Problem: impurities decrease efficiency
- μ-XRF and μ-XAFS to characterize metal precipitates and suggest processing to improve efficiency

μ-XRF & μ-XAFS: two defects

~ 20 nm silicide

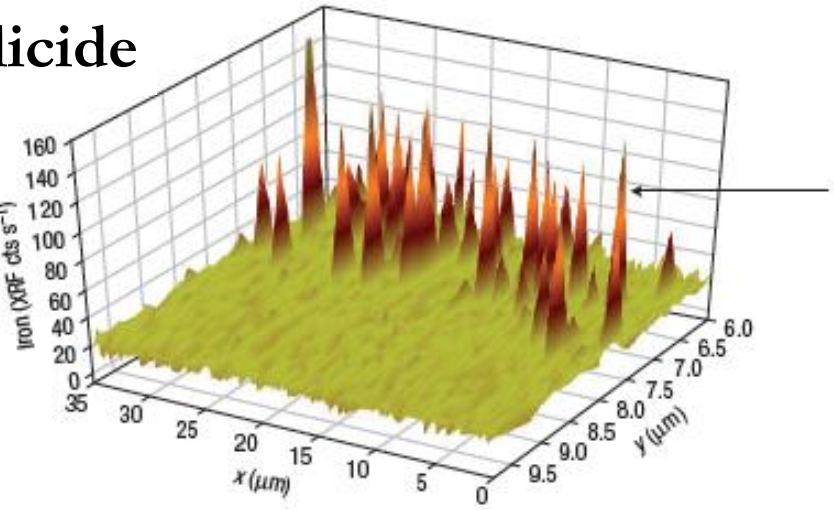

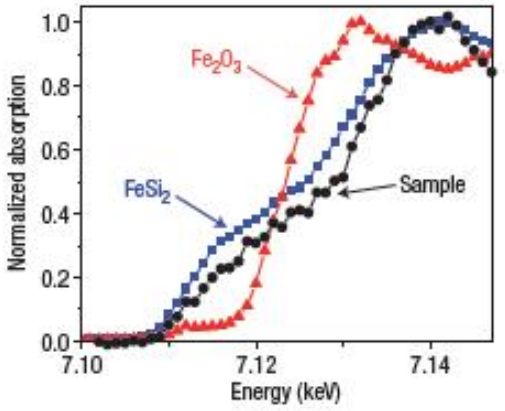

~ 10 μm oxide

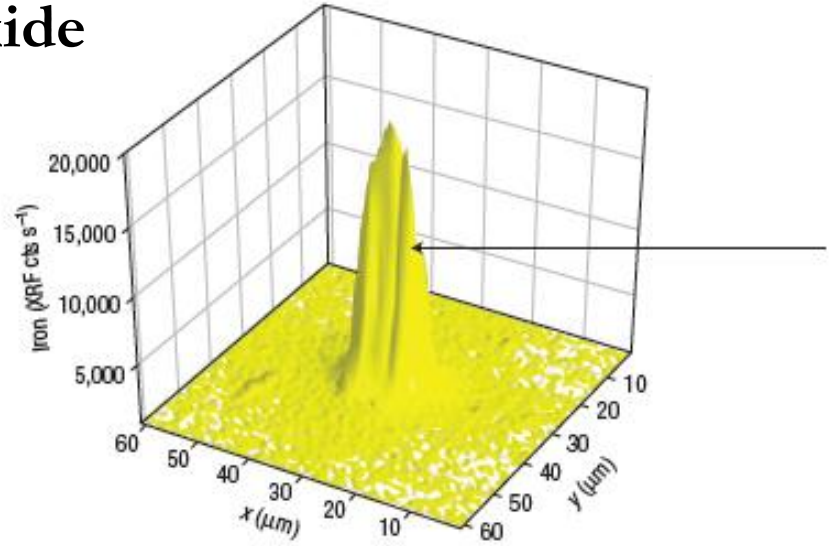

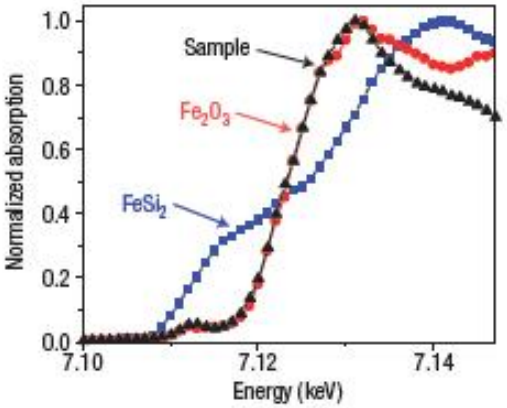

Processing & characterization

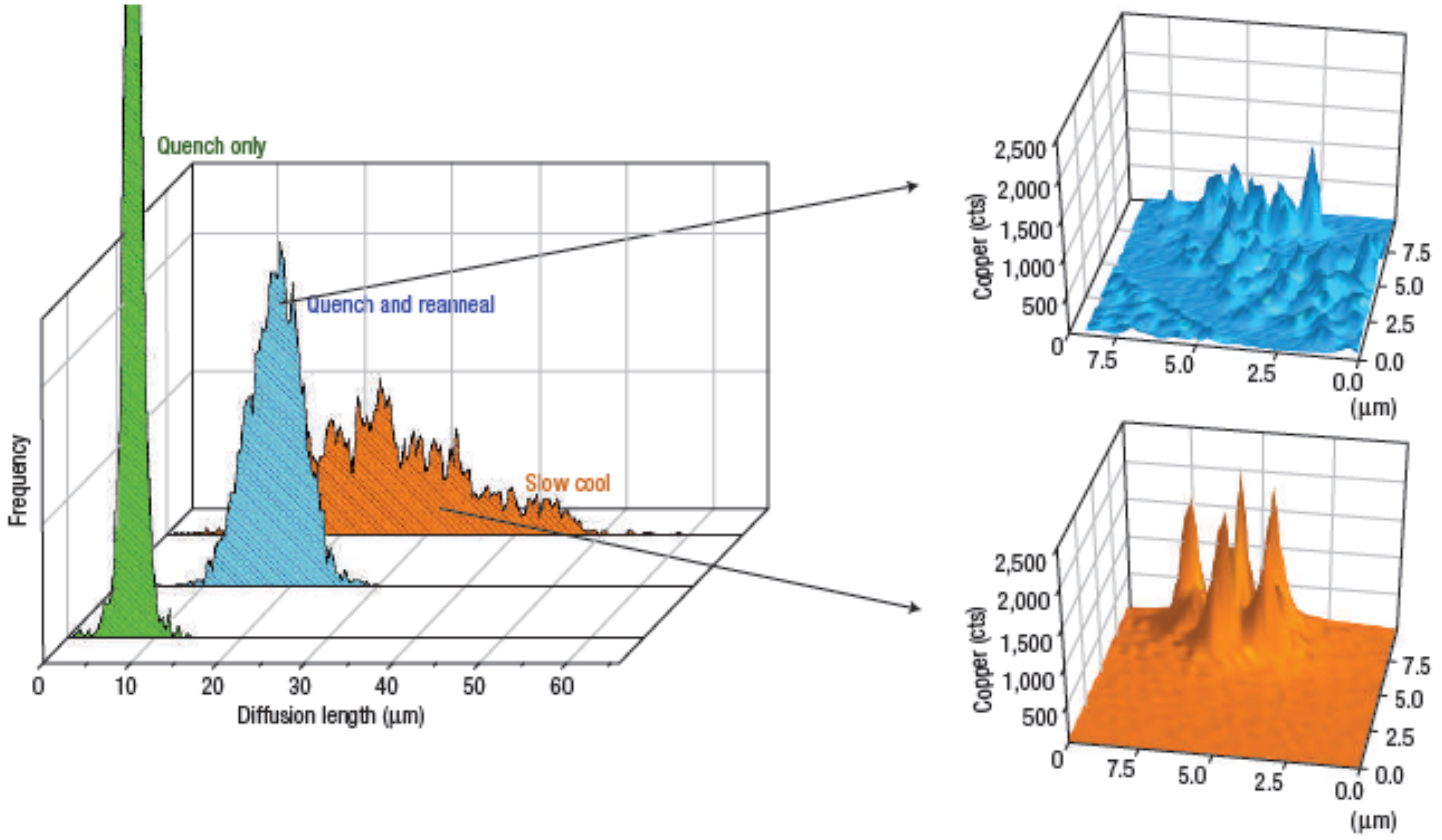

Best process: slow cool (5 °C s^{-1}) from 1200 °C

µm sized, low density precipitates lead to greater carrier diffusion lengths

Low Z dopants and XAS

- C, N & O often used as dopants
- Experimentally difficult: low fluorescence yield, soft X-rays, UHV

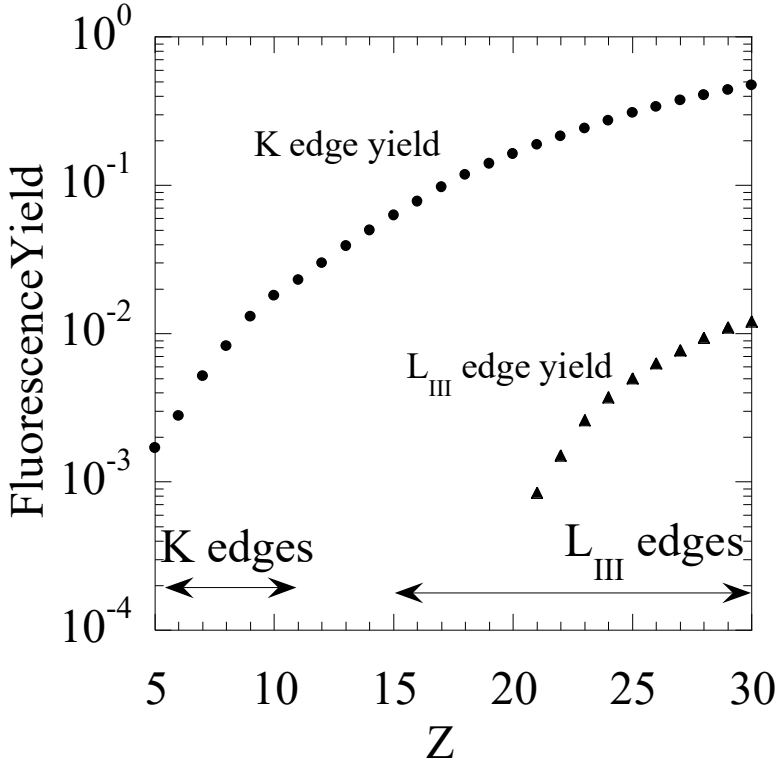

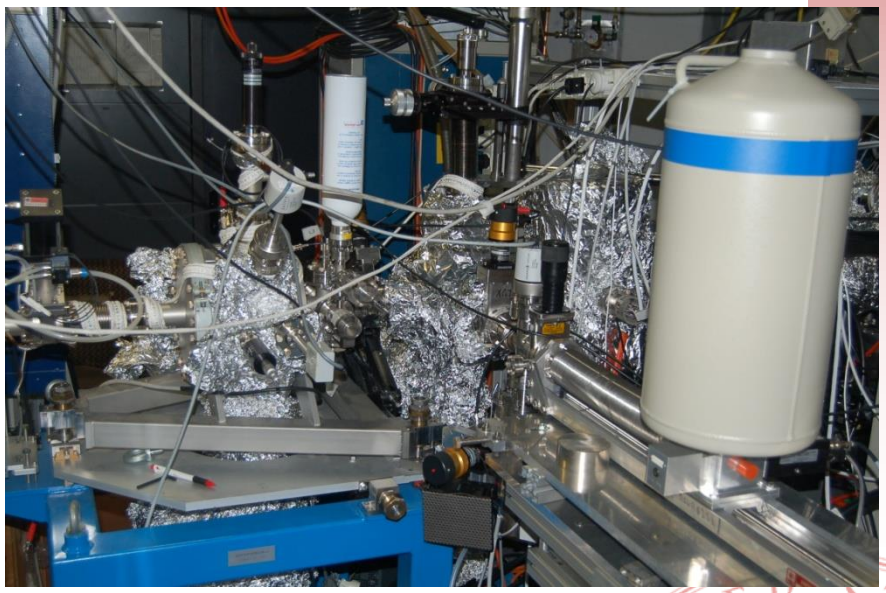

ALOISA beamline @ ELETTRA

Dilute nitrides: $GaAs_{1-y}N_y$, $In_xGa_{1-x}As_{1-y}N_y$

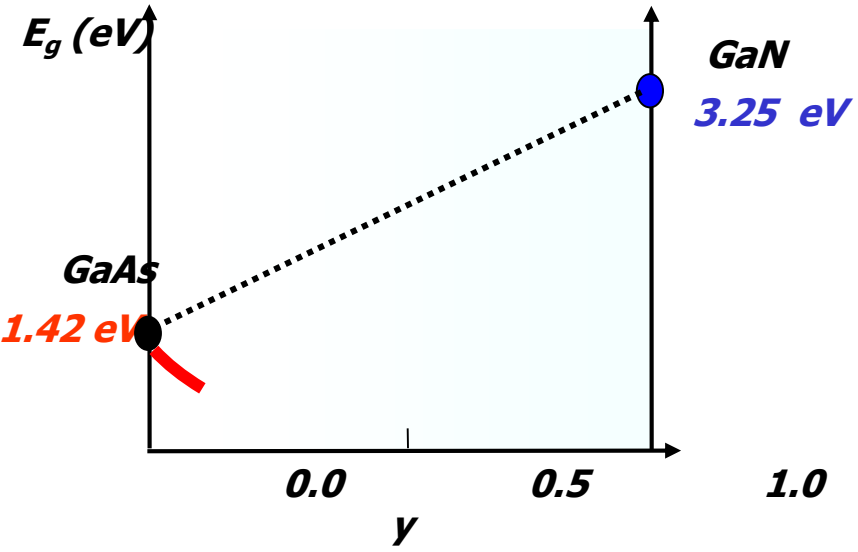

- Anomalous non-linear optical and electronic proprieties of III-V nitrides
- Red shift of the band gap by adding few % of nitrogen (≈ 0.05-0.1 eV per N atomic percent in InGaAsN)
- Huge and composition dependent optical bowing

Hydrogen – nitrogen complexes in dilute nitrides

- Hydrogenation leads to reversible opening of E_g

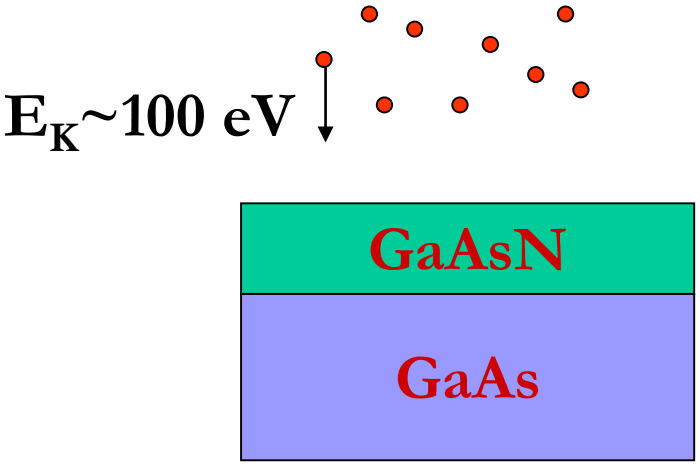

photoluminescence

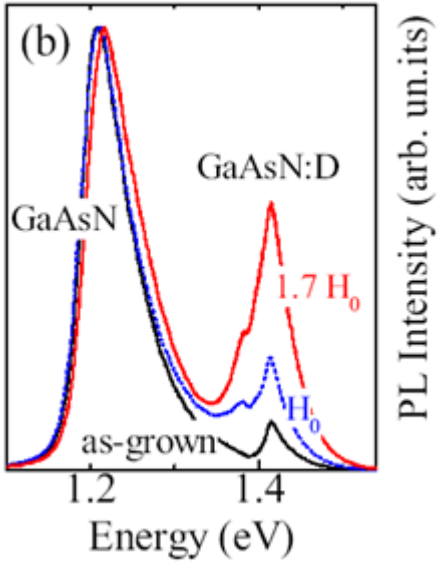

Hydrogen – nitrogen complexes in dilute nitrides

- Which is the hydrogen –nitrogen complex responsible for these changes?

Some candidate low energy structures

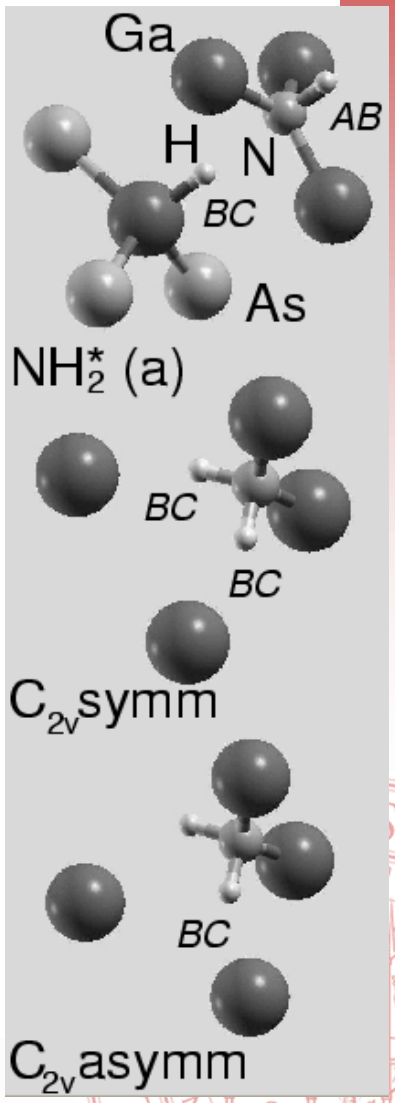

H– N complexes in dilute nitrides

- G. Ciatto, F. Boscherini, A. Amore Bonapasta, F. Filippone, A. Polimeni and M. Capizzi, Phys. Rev. B **71**, 201301 (2005)
- M. Berti, G. Bisognin, D. De Salvador, E. Napolitani, S. Vangelista, A. Polimeni, M. Capizzi, F. Boscherini, G. Ciatto, S. Rubini, F. Martelli, and A. Franciosi, Phys. Rev. B **76**, 205323 (2007)
- G. Ciatto, F. Boscherini, A. Amore Bonapasta, F. Filippone, A. Polimeni, M. Capizzi, M. Berti, G. Bisognin, D. De Salvador, L. Floreano, F. Martelli, S. Rubini, and L. Grenouillet, Phys. Rev. B **79**, 165205 (2009)

- DFT calculations to determine lowest energy geometries
- Full multiple scattering XANES simulations
- Answer: C_{2v} – like complexes are mostly present
- 3-D sensitivity of XANES!!

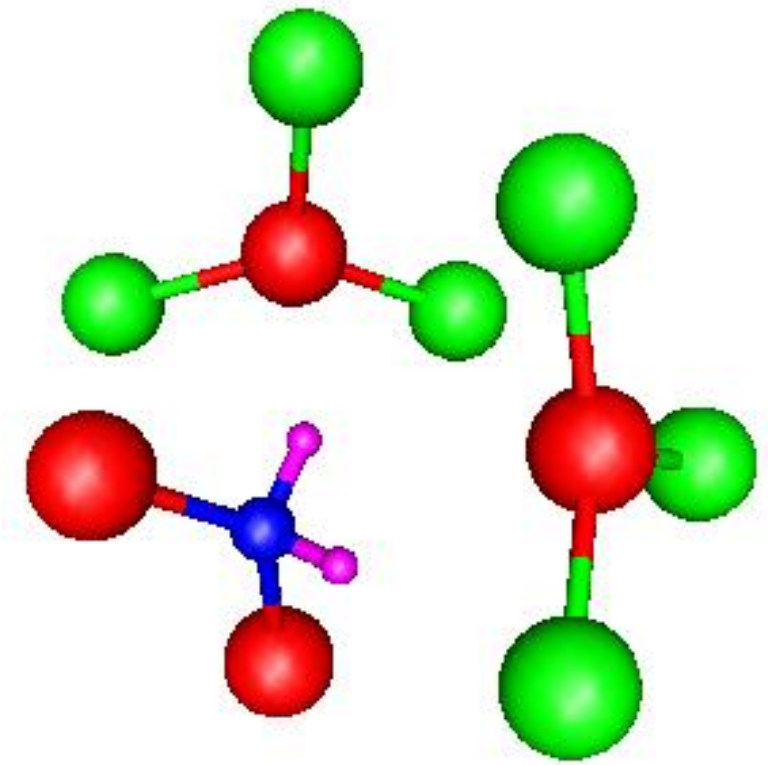

Combined XAFS and XES

Amidani et al., Phys. Rev. B 89, 085301 (2014)

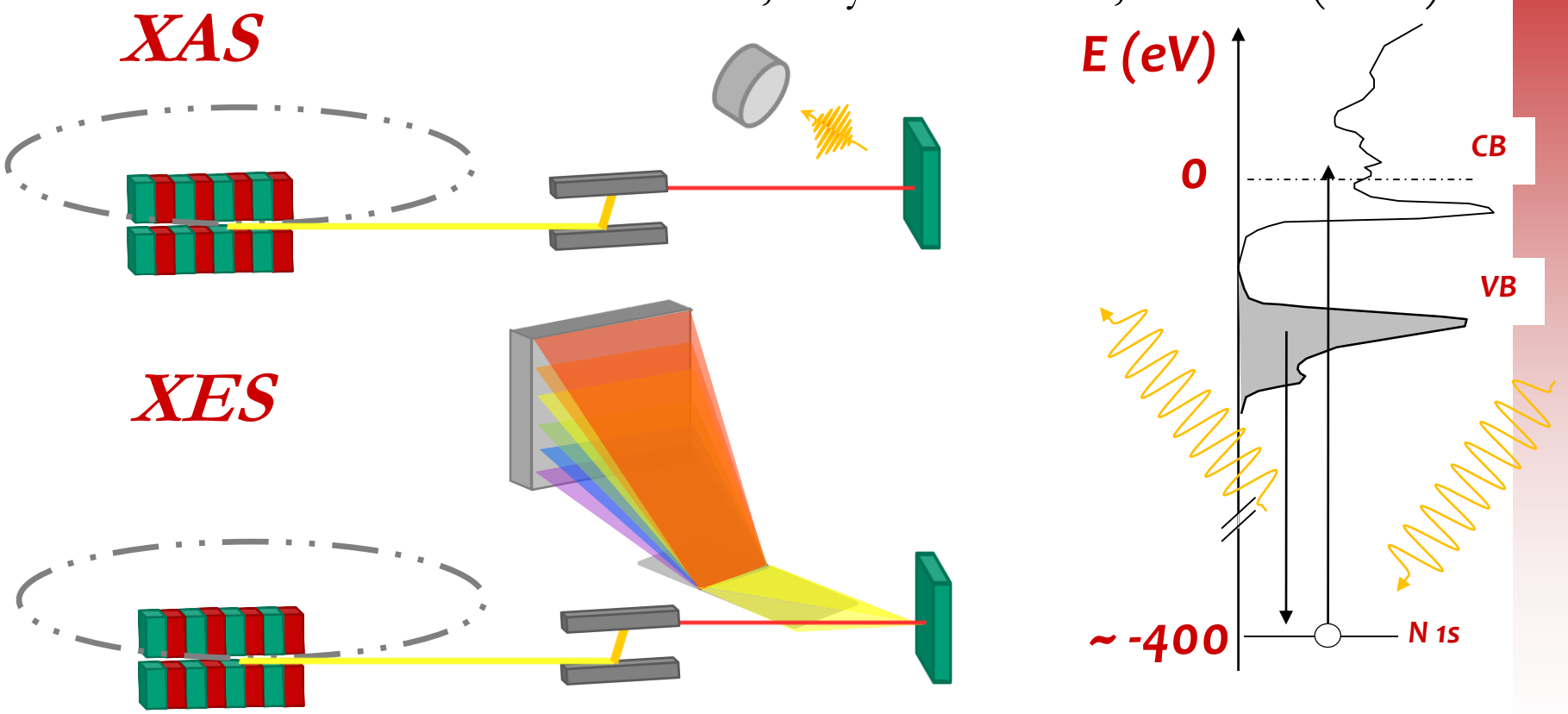

XES now possible, a complementary tool with sensitivity to

- Valence band electronic structure
- Atomic structure
- New level of refinement in x-ray spectroscopy

Combined XAFS and XES

XES

- local VBM unchanged
- decrease of main peak in favor of lower energy states

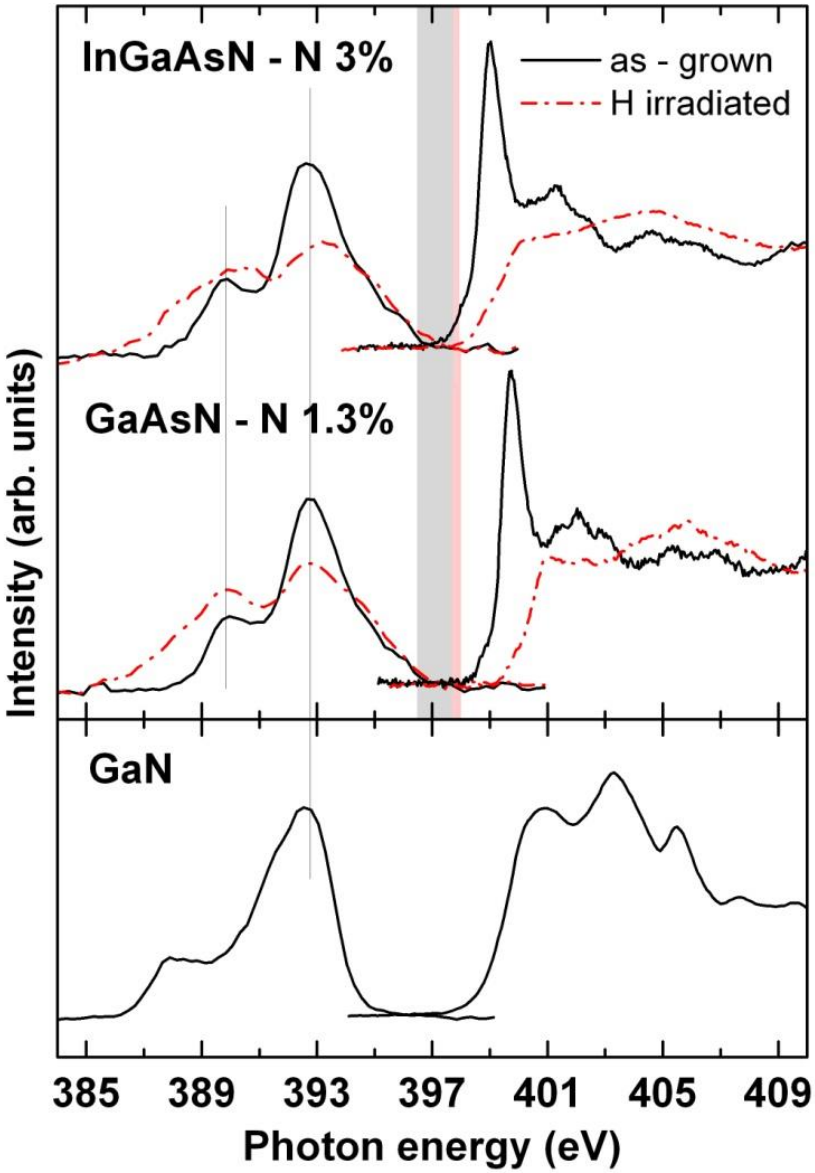

XAFS

- main peak disappears and local CBM is strongly blue-shifted
- N states move far from the CBM

XAFS and XES simulations

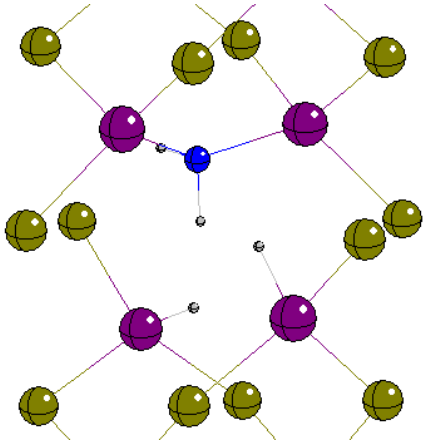

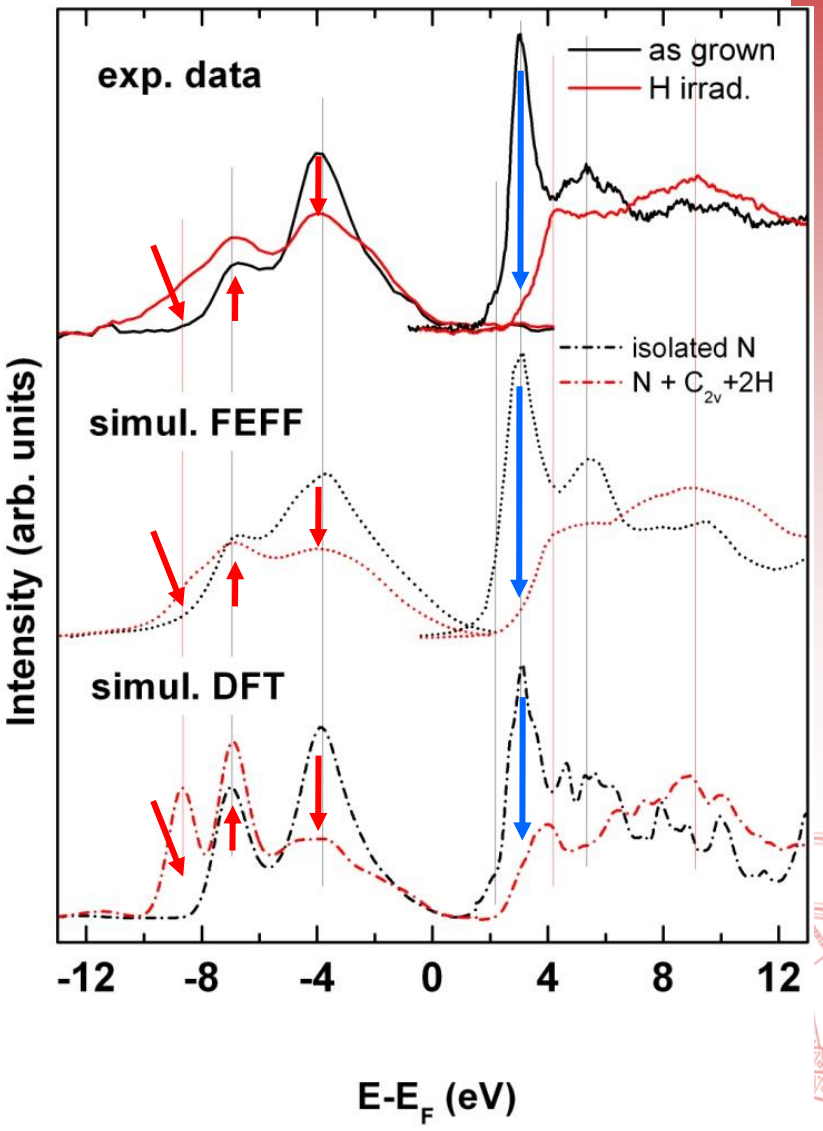

Good news: all spectral features are well reproduced by:

- MS spectral simulations based on DFT atomic structure
- ab-initio DFT simulations of electronic and atomic strcuture

XAFS and alloys

- High resolution in probing the local coordination in first few coordination shells
- Study, as a function of composition
  - Deviation of local structure from average structure
  - Atomic ordering

Semiconductor alloys

- For example: $In_xGa_{1-x}As$
- Alloying leads to changes in
  - band-gap
  - lattice parameter

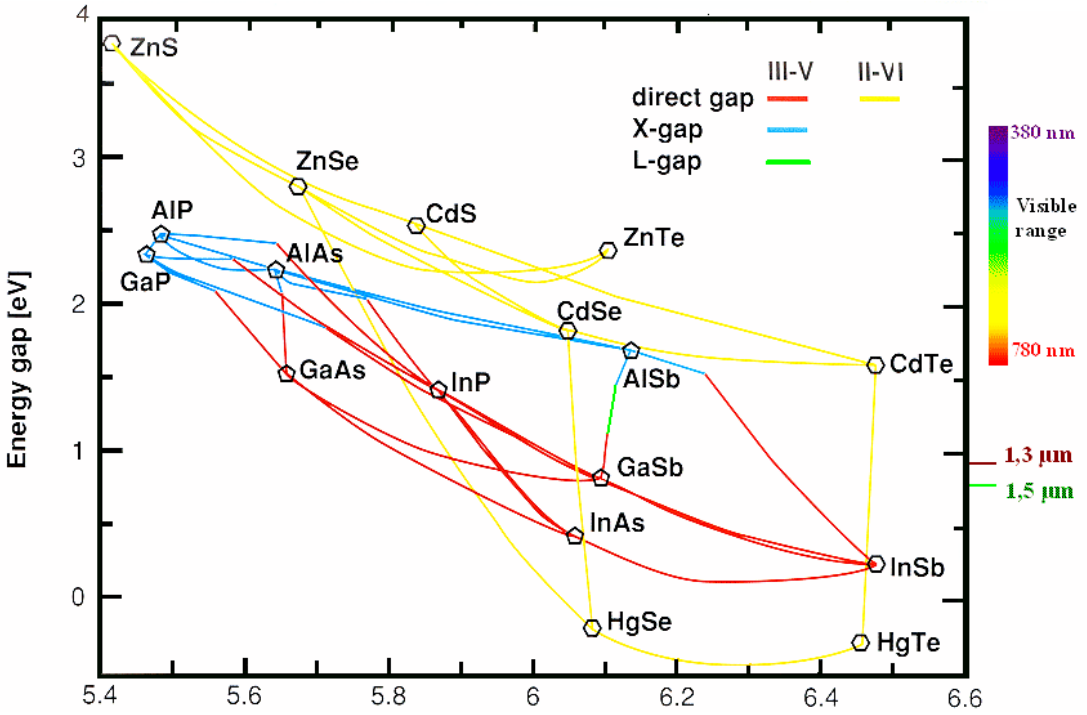

Vegard's law & Virtual Crystal Approximation

- The lattice parameter depends linearly on concentration: "Vegard's law"
- VCA: a linear and isotropic variation of the local structure with concentration
  - All atoms retain symmetric tetrahedral bonding

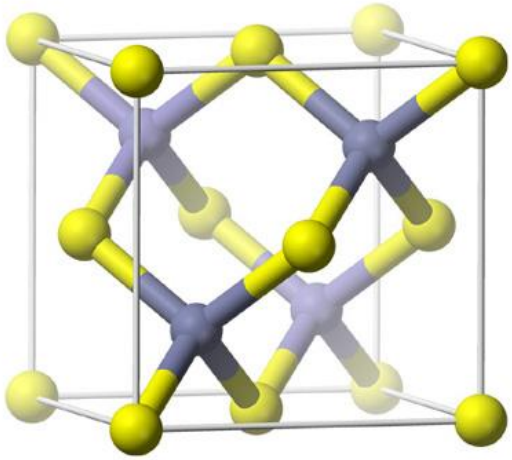

GaAs

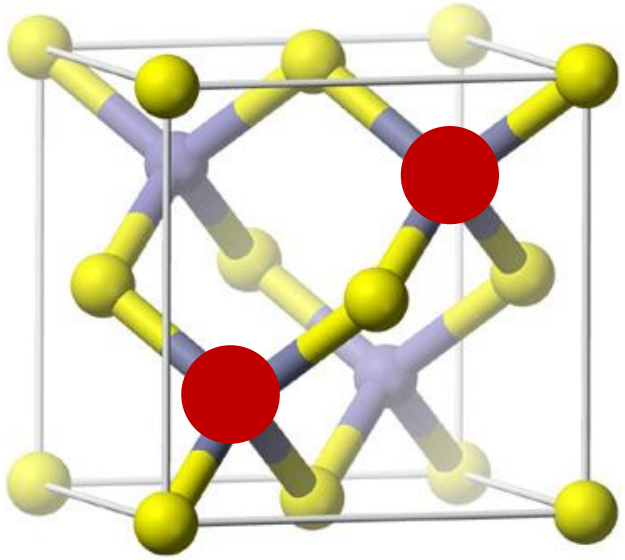

$In_{0.5}Ga_{0.5}As$

Bond lengths in $In_xGa_{1-x}As$

- The high resolution of EXAFS in determining bond lengths (0.01 Å) has shown that they stay close to sum of covalent radii
- Violation of the VCA
- First evidence of strong local structural distortions
- Mikkelsen Jr. and Boyce, Phys. Rev. Lett. **49**, 1412 (1982)

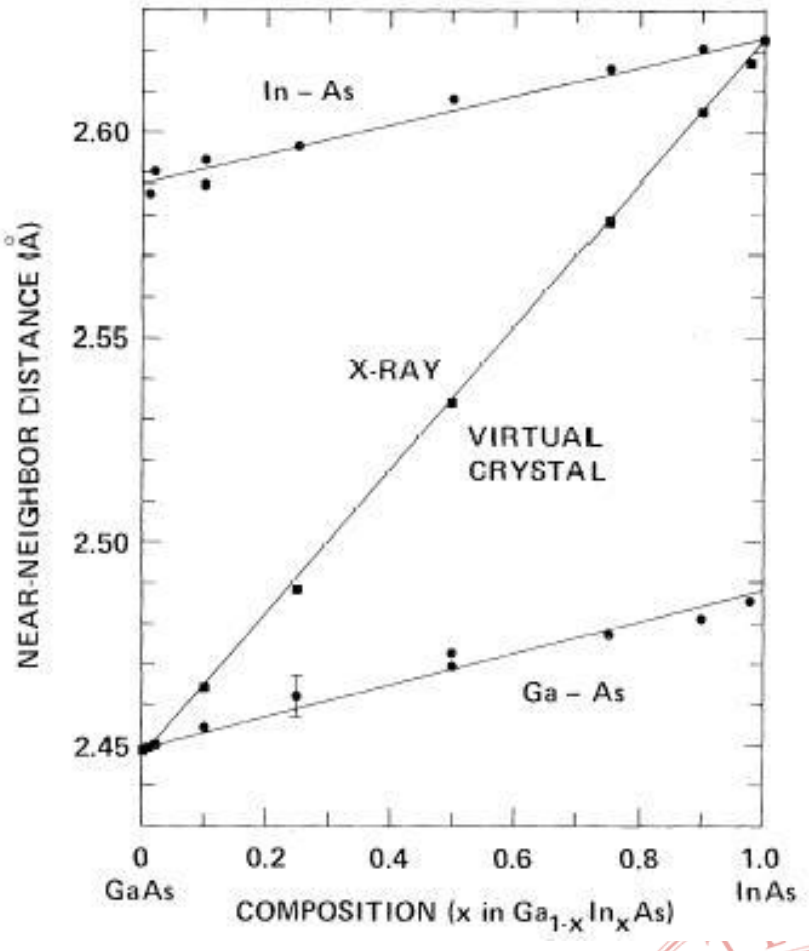

Origin of local structural distortions

- Local deformation potential:

$$V(\{R_{ij}\},\ \{\theta_{ijk}\}) =$$

$$\frac{\alpha}{2}\sum_{ij}(R_{ij}-R_{ij}^{0})^{2}+\frac{\beta}{8}\,R_{e}^{2}\sum_{ijk}(Cos\,\theta_{ijk}+\tfrac{1}{3})^{2}$$

- For most semiconductors $\alpha \gg \beta$
  - The covalent bond is stiff and directional

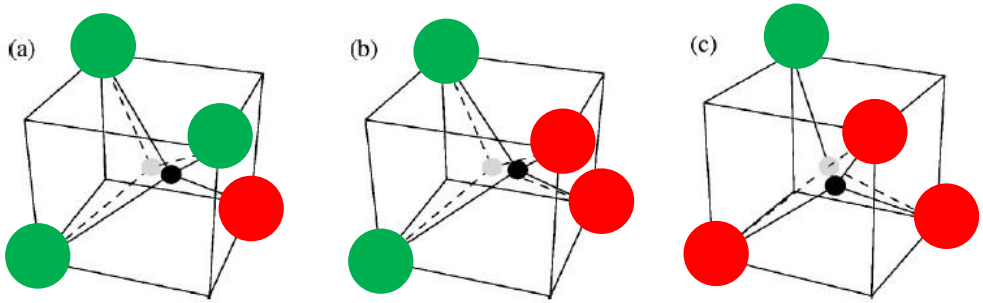

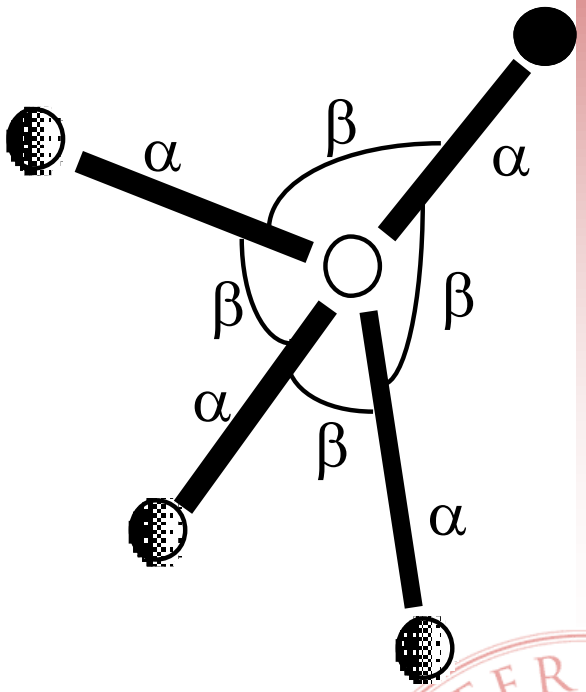

$Ga_{1-x}In_xP$ alloys

C. S. Schnohr, L. L. Araujo, P. Kluth, D. J. Sprouster, G. J. Foran, and M. C. Ridgway, Phys. Rev. **78**, 115201 (2008)

- 26 years later
  - Much better data
  - More sophisticated analysis
- Same conclusion!

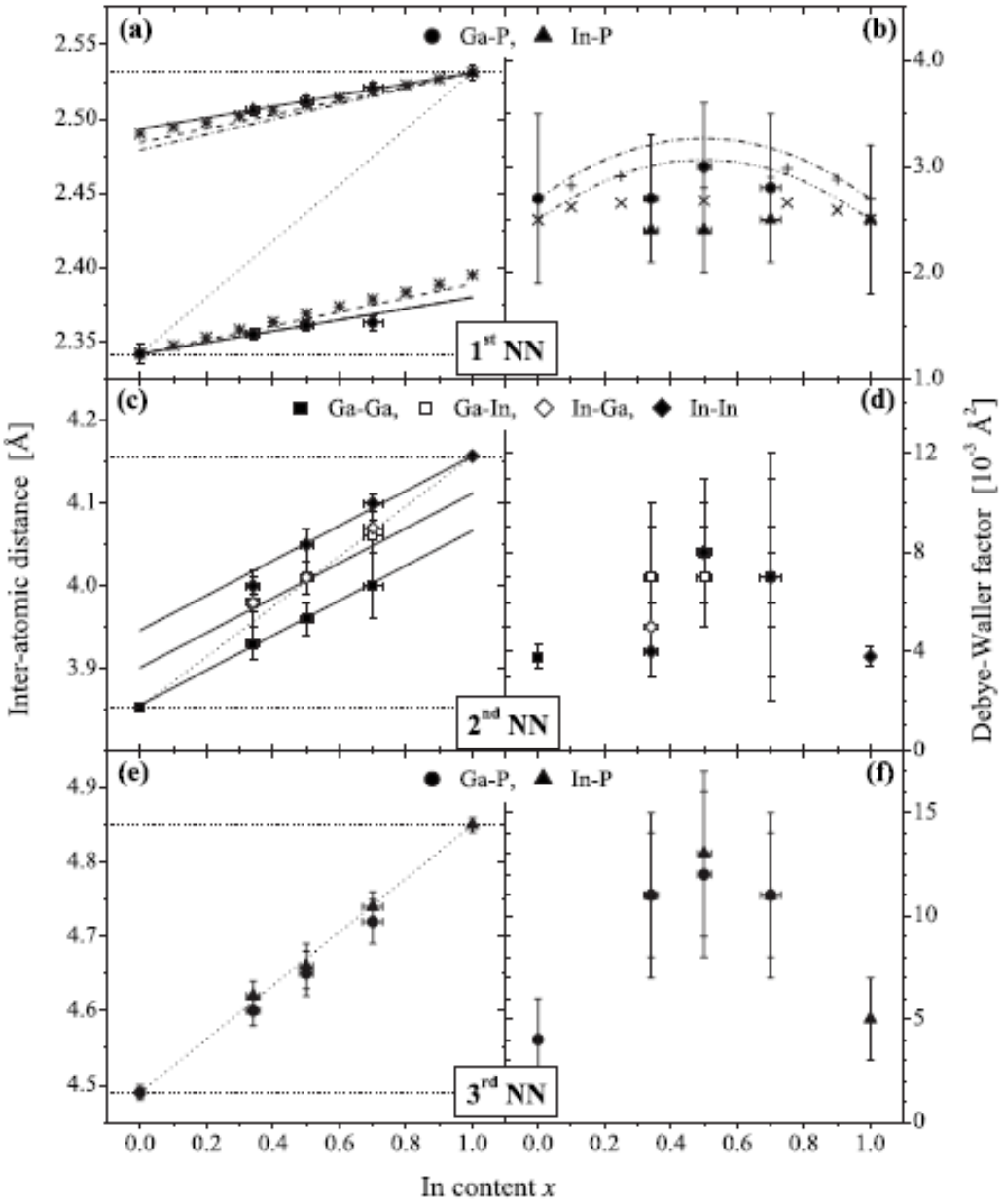

XAFS and phase transitions

- Measure local structure through the phase transition
- XAFS has highlighted the difference between the real local structure and the average structure

Ferroelectric Phase transitions in $PbTiO_3$

Sicron, Ravel, Yacoby, Stern, Dogan and Stern, Phys. Rev. B 50, 13168 (1994)

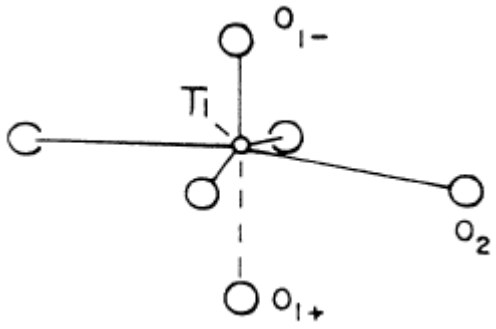

low temp

- At T_c = 763 K $PbTiO_3$ undergoes tetragonal to cubic phase transition
- $T < T_c$ it is ferroelectric (permanent dipole moment)
- Phase transition believed to be purely displacive (no local distortion for $T > T_c$)

Ferroelectric Phase transitions in $PbTiO_3$

- Ti and Pb XAFS data
- "Local lattice parameters" and local distortions do not change at T_c
  - *c*: sum of R(Ti-O_1)
  - *a*: calculated from R(Ti-O_2)
- Conclusion
  - local distortions survive above T_c
  - Above Tc random orientation of domains with permanent dipole moment

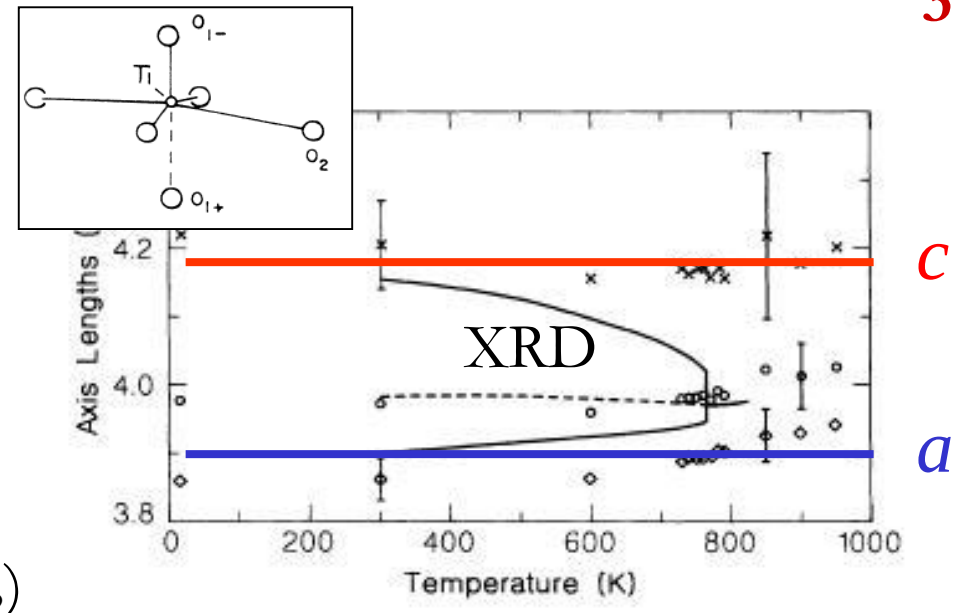

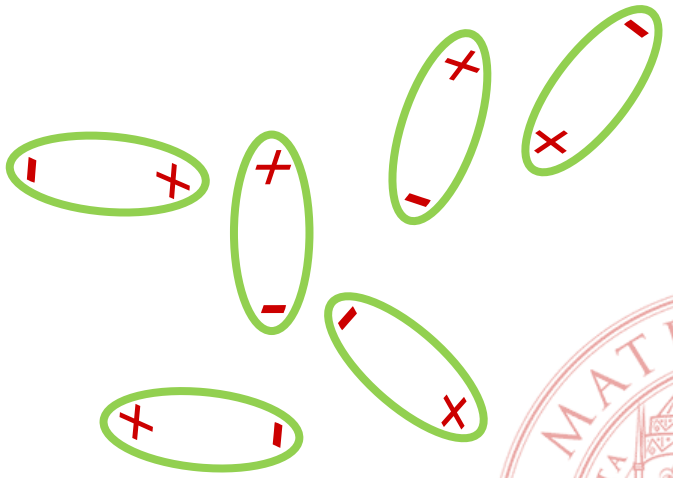

Phase change mechanism in optical media

Kolobov et al., Nature Materials **3**, 703 (2004)

- Phase change optical discs used in DVD-RAMs are based on $Ge_2Sb_2Te_5$ (GST)
- Writing: appropriate laser pulses induce reversible phase changes from amorphous to crystalline
- Reading: the reflectivity of the two phases is different
- What is associated structural change?

Phase change mechanism in optical media

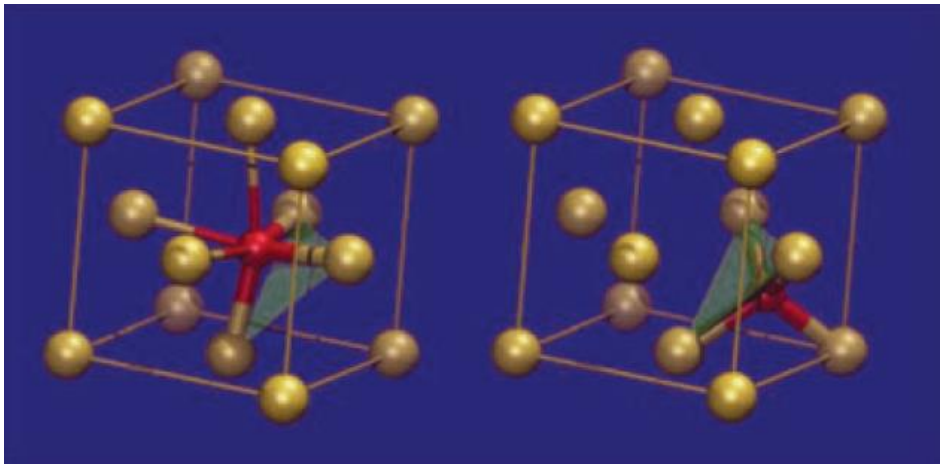

- Phase change is based on "umbrella flip" of Ge, from octahedral to tetrahedral coordination within Te fcc lattice
  - Three strong Ge – Te covalent bonds remain intact
  - Weaker Ge – Te bonds are broken by laser pulse
- Phase change in GST is fast and stable because the process does not require rupture of strong bonds or diffusion

Time resolved XAFS of phase change

Fons et al., Phys. Rev. B **82**, 041203 (2010)

- Sub nanosecond time resolved XAFS with μm spot size at SPring-8
- The intensity of the "white line" is different for crystalline, amorphous and liquid phases

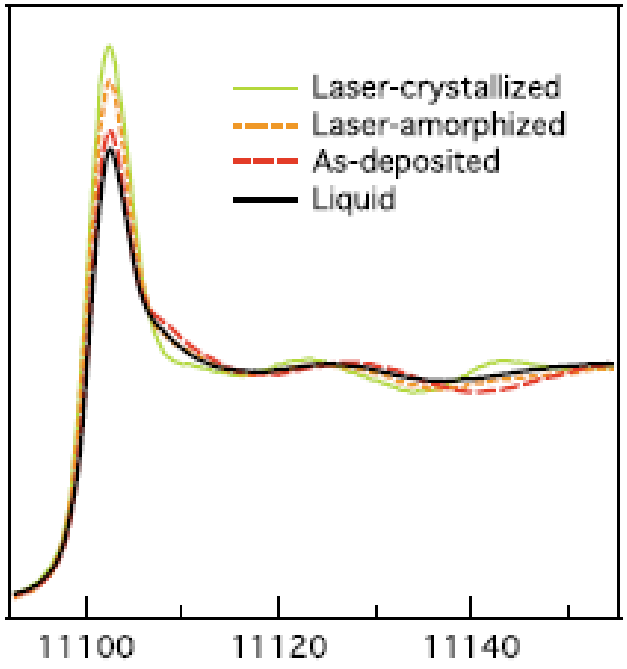

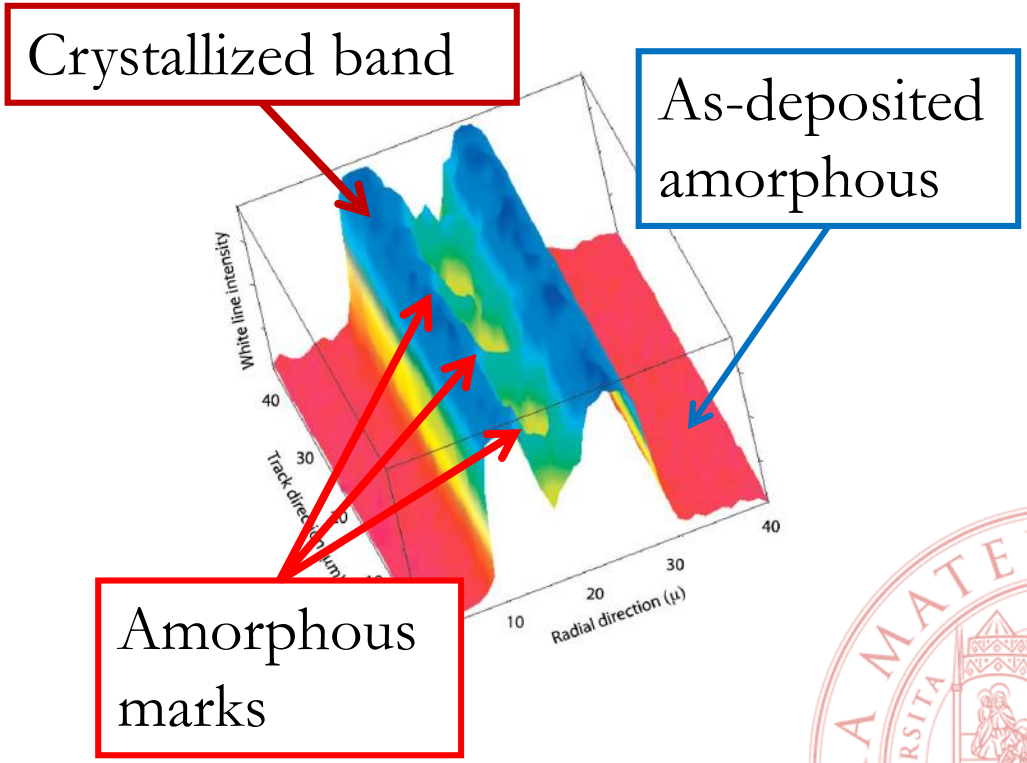

Time resolved XAFS of phase change

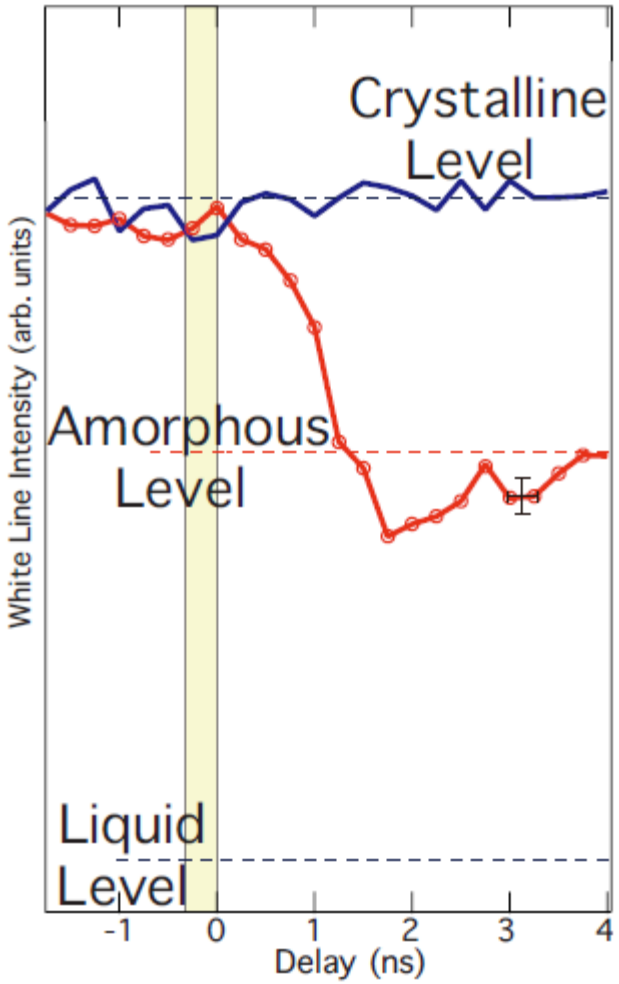

- White line intensity versus time
  - 100 ps time resolution
- Phase change does not involve melting

XAFS and thin films / interfaces

- With specific detection schemes sensitivity to very thin films achievable
  - Grazing incidence
  - Electron / fluo detection
- Exploit linear polarization of SR to obtain information on
  - Orientation
  - Lattice symmetry

Cubic and hexagonal GaN

- N K-edge XAS to study relative amounts of cubic and hexagonal GaN
- Exploit
  - linear polarization of SR
  - polarization dependence of cross-section
- XAS signal must exhibit (at least) point group symmetry of the crystal
  - T_d: isotropic signal
  - C_{6V}:

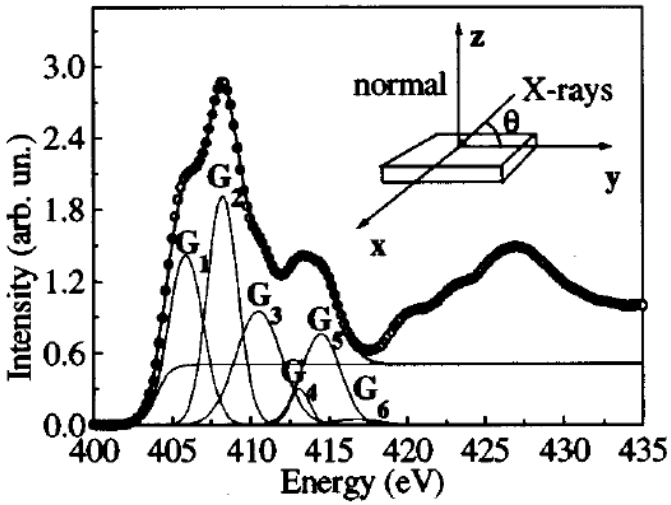

$$\sigma^{tot}(E,\theta)=\sigma^{iso}(E)+(3Cos^2\theta-1)\sigma^{1}(E)$$

GaN

CUBIC

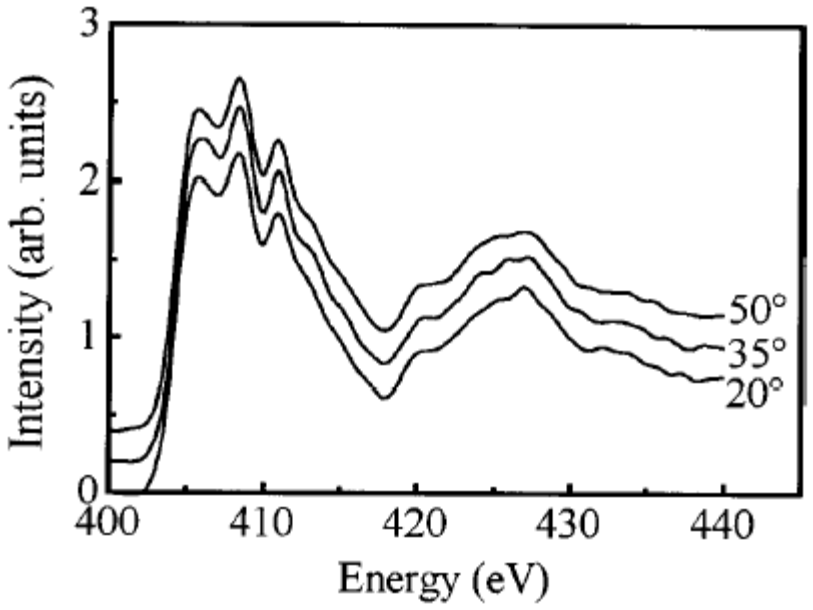

HEXAGONAL

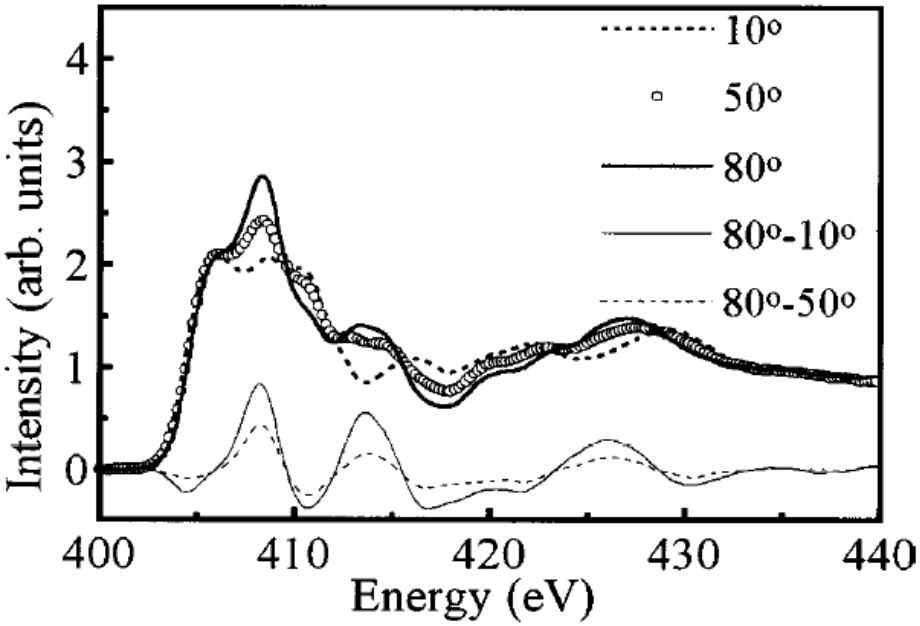

- Katsikini et. al., APL **69**, 4206 (1996); JAP **83**, 1440 (1998)

C K edge XANES

- Transitions to π^* molecular orbitals give rise to strong peak

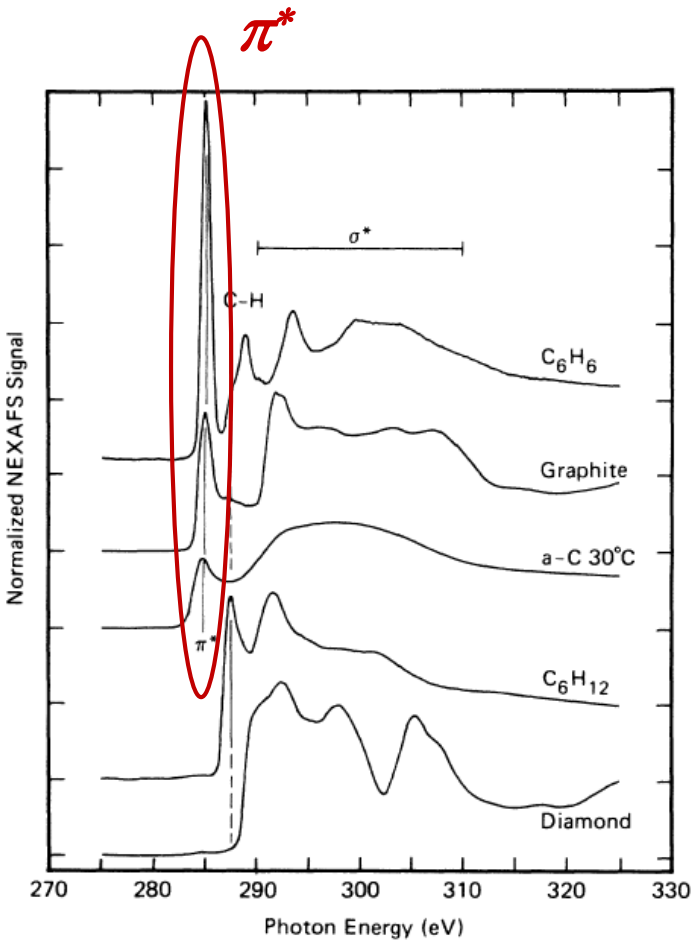

Comelli et al., Phys. Rev. B 38, 7511 (1988)

Use of linear dichroism

- Intensity of peaks related to transitions to π* orbitals depends on the orientation between the orbital and $\vec{E}$

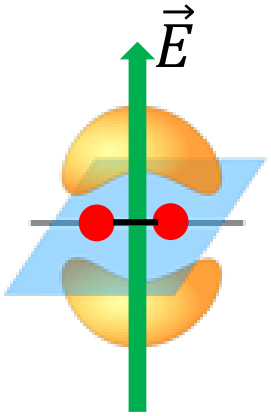

Maximum intensity

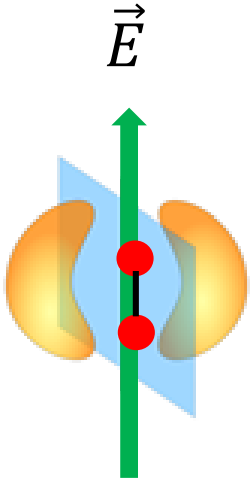

Minimum intensity

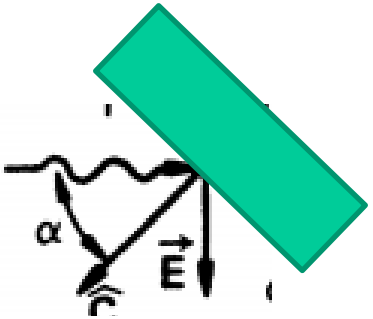

C K edge XANES of graphite

- Very clear dependence of peak due to transitions to π^* orbitals on orientation
- π^* are perpendicular to surface plane
- Rosenberg et al, Phys. Rev. B33, 4034 (1986)

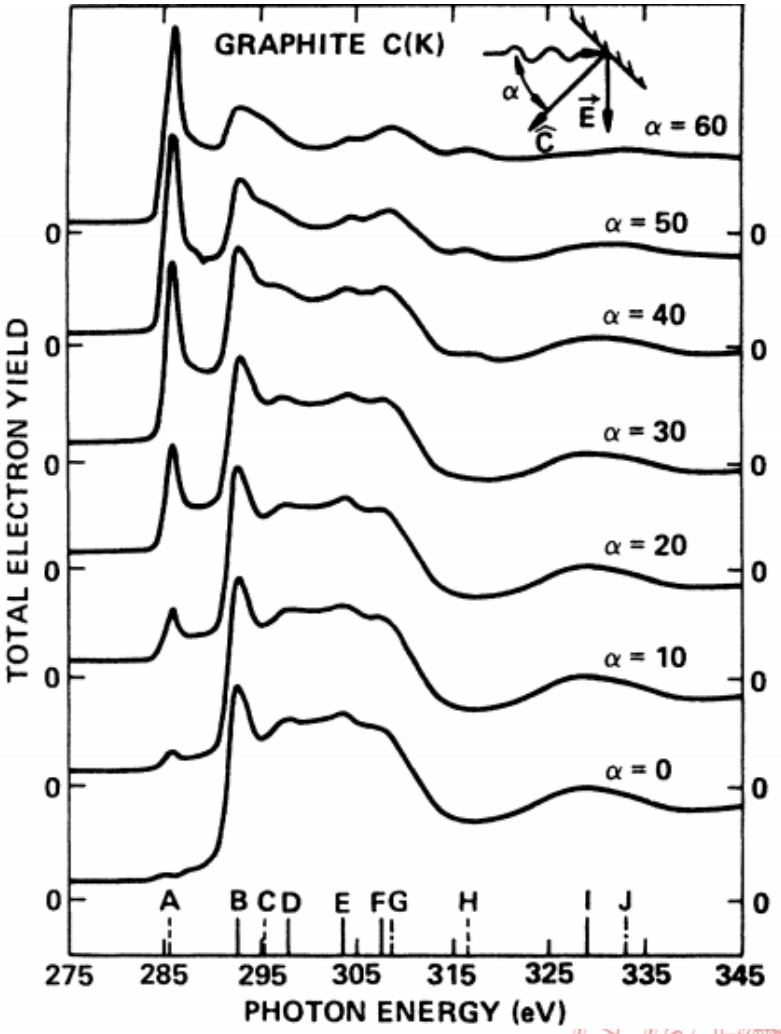

Orientation of molecules on surfaces

- Typical application: determination of the orientation of molecules on single crystal surfaces
- N_2 on Ni(110)
- Molecules are "vertical"

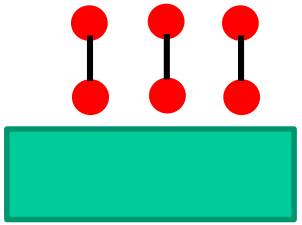

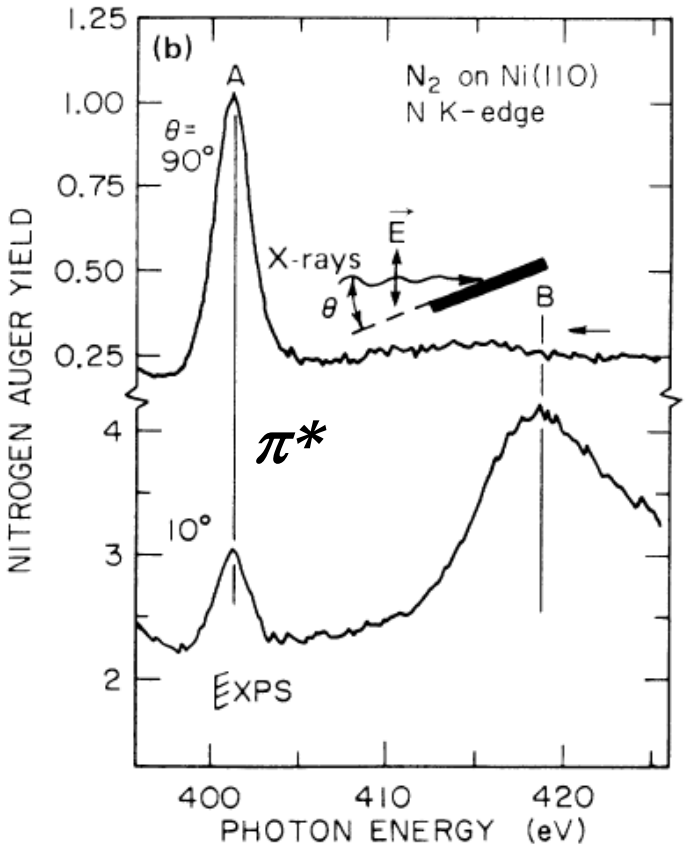

Stöhr & Oukta, Phys. Rev. B 36, 7891 (1987)

The Fe/NiO(001) interface

P. Luches, V. Bellini, S. Colonna, L. Di Giustino, F. Manghi, S. Valeri, and F. Boscherini, Phys. Rev. Lett. 96, 106106 (2006).

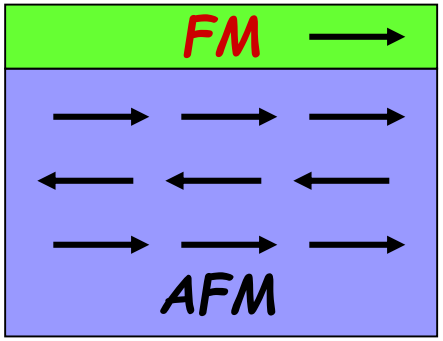

heating up to T_N

+

cooling in H

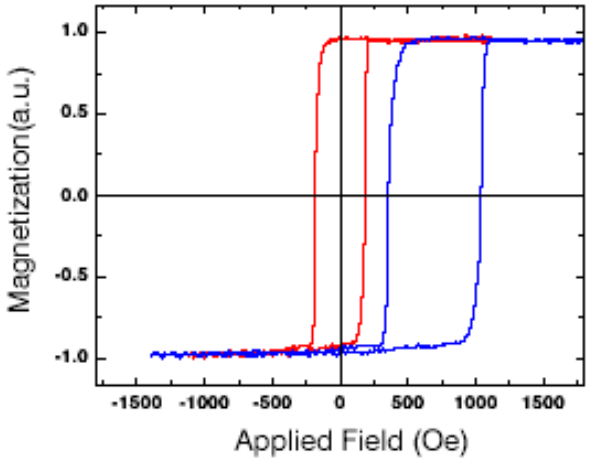

exchange bias

The Fe/NiO(100) interface

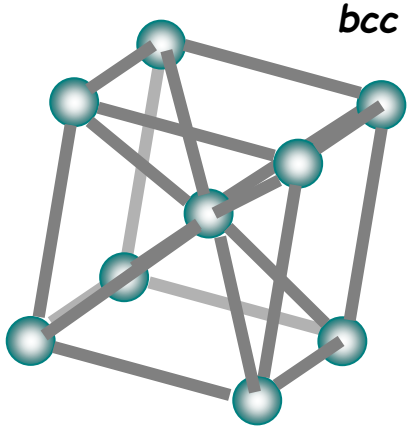

Fe

FM T_C=1040 K

a_{Fe}= 2.866 Å

m= - 2.8%

d_{Fe} = 4.053 Å

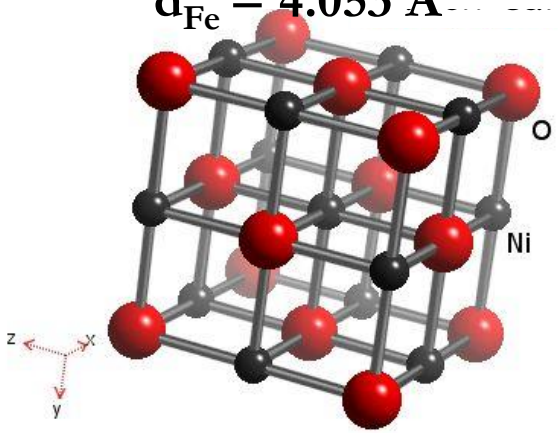

NiO

AF T_N=520 K

a_{NiO}= 4.176 Å

Fe/NiO XANES

- deviation from metallic character

- shift of the white line towards FeO

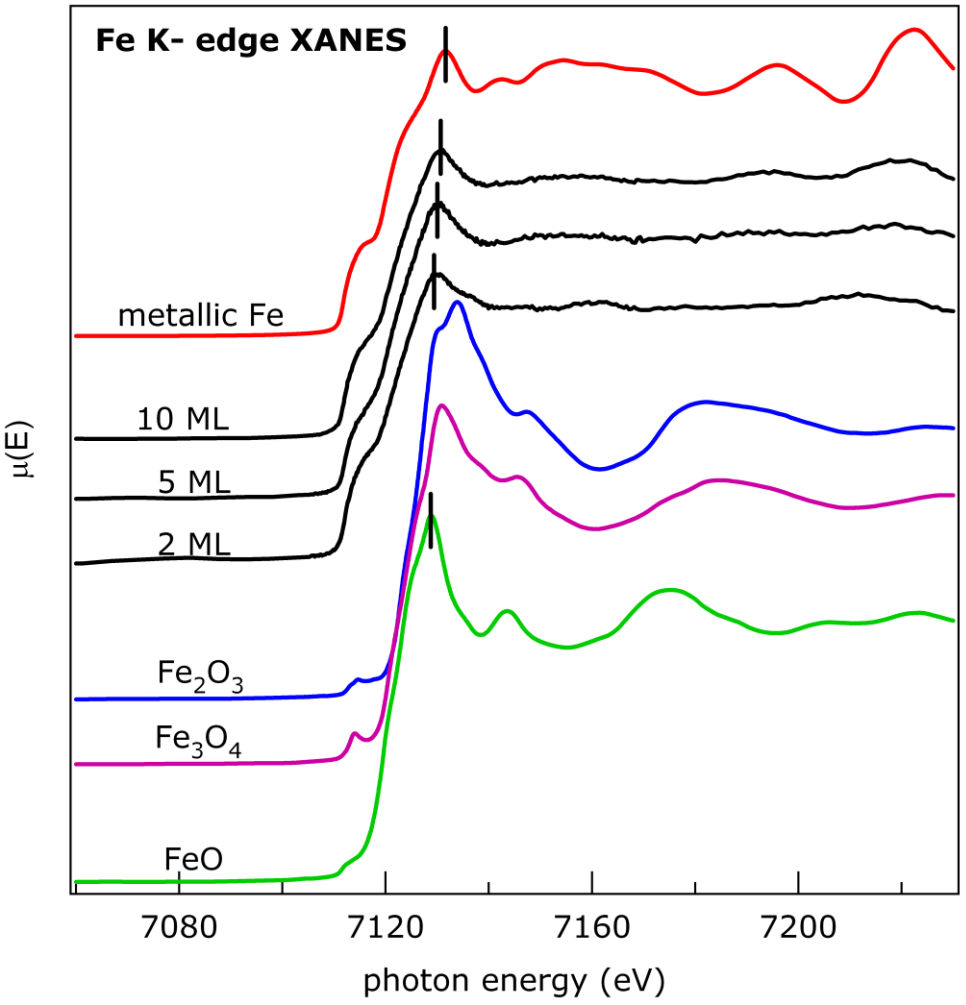

Fe/NiO XANES: polarization dependence

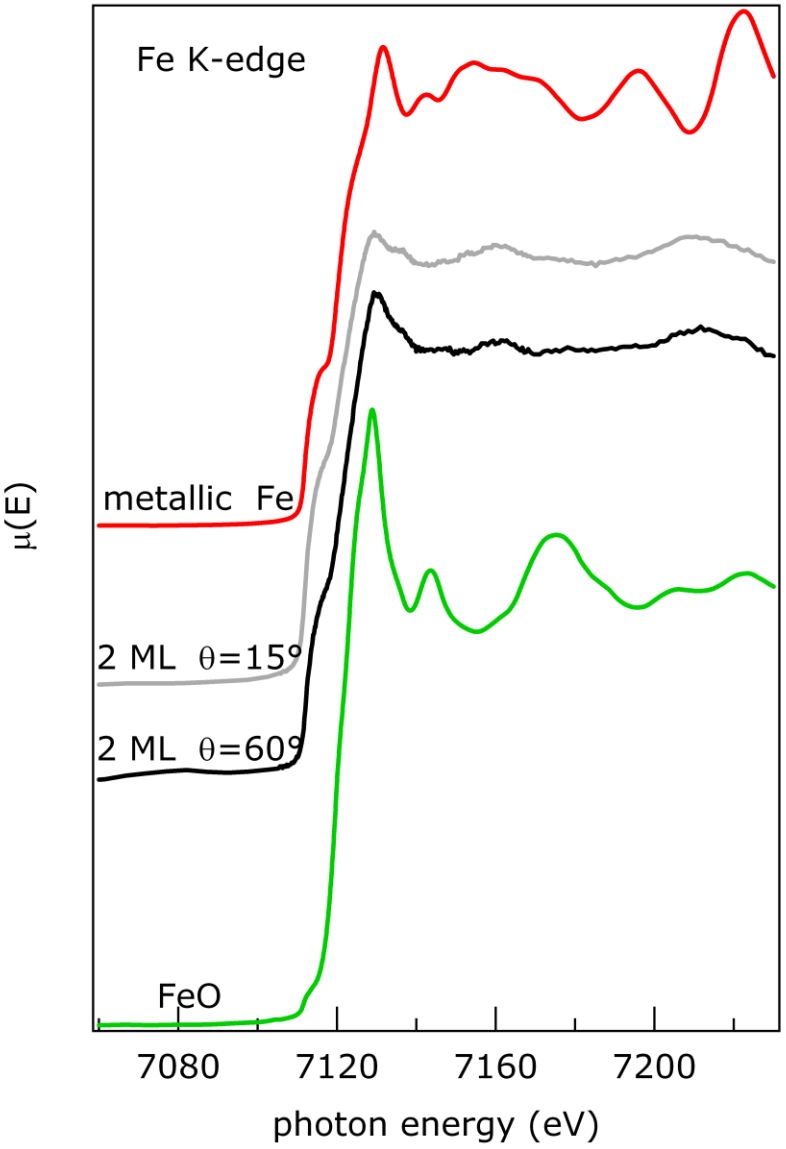

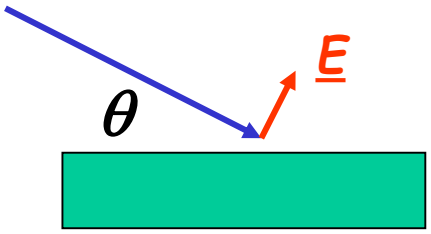

planar FeO phase

Fe/NiO 2 ML thickness

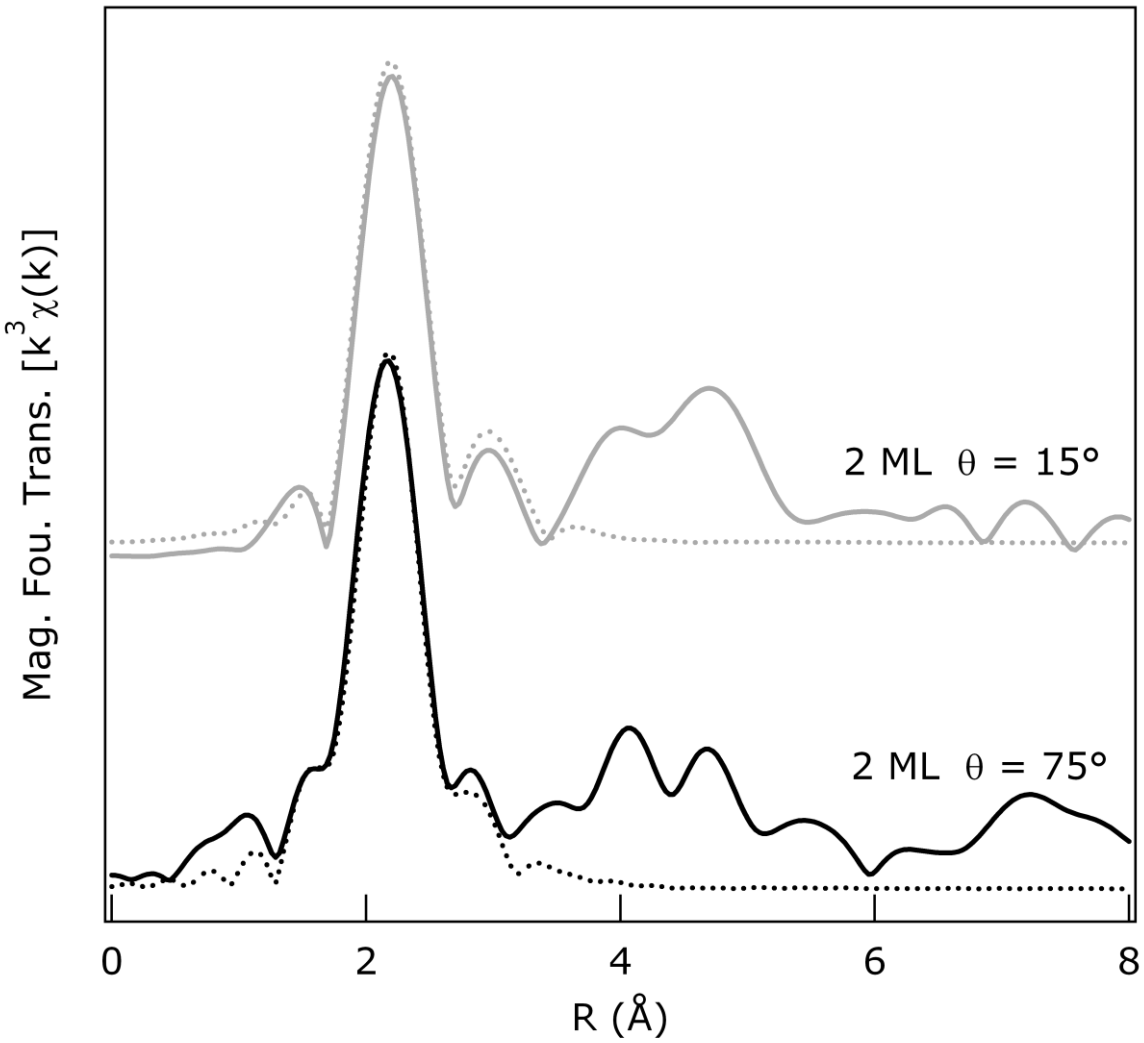

Fe/NiO: atomic structure of interface

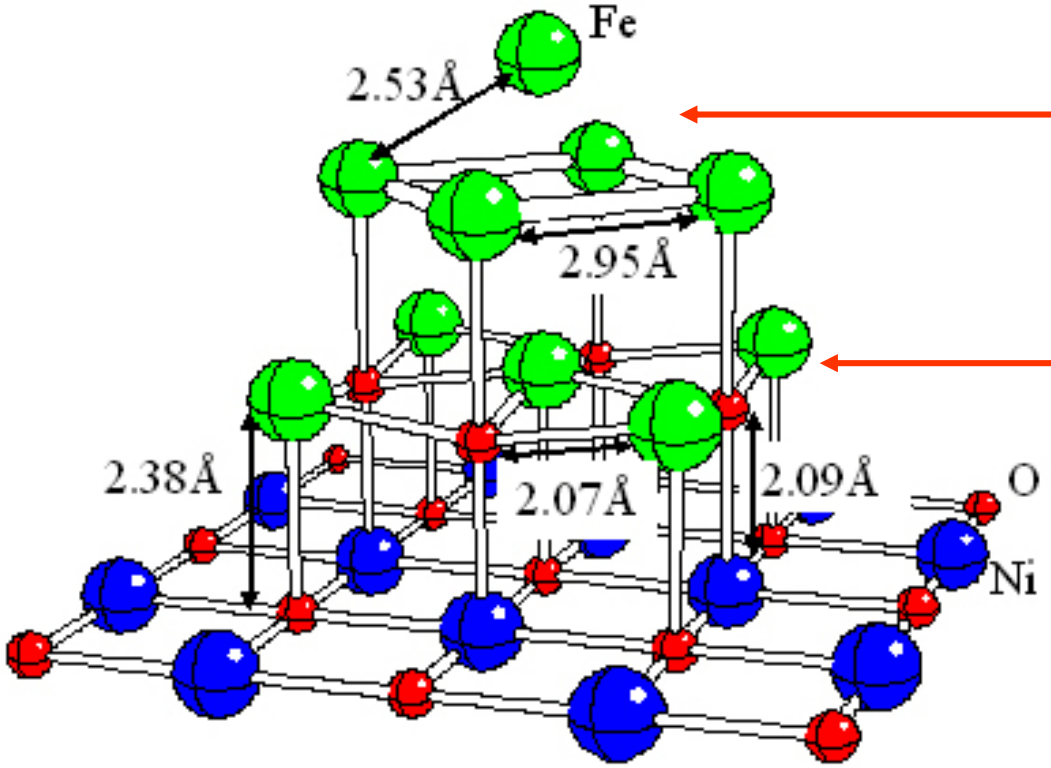

BCT Fe

buckled pseudomorphic FeO layer

- expanded FeO-NiO and FeO-Fe distance

XAFS and nanostructures

- XAFS is a local, short range, effect
  - Origin: core hole lifetime (t_{hole} = 10^{-16} – 10^{-15} s) and electron mean free path (5 – 10 Å).
- Same formalism applies to molecule, cluster or crystalline solid
  - insenstive to variations of morphology
  - sensitive to low thicknesses, high dilutions
- Excellent probe of variations in local environment due to
  - Size effects
  - Change 3D / 2D / 1D

Ge Quantum Dots

F. Boscherini, G. Capellini, L. Di Gaspare, F. Rosei, N. Motta, and S. Mobilio, Appl. Phys. Lett. **76**, 682 (2000)

- Need for understanding of local bonding
- Preparation:
  - Ge/Si(001) by CVD @ 600 °C, Univ. Roma Tre
  - Ge/Si(111) by MBE @450 - 550 °C, Univ. Roma II

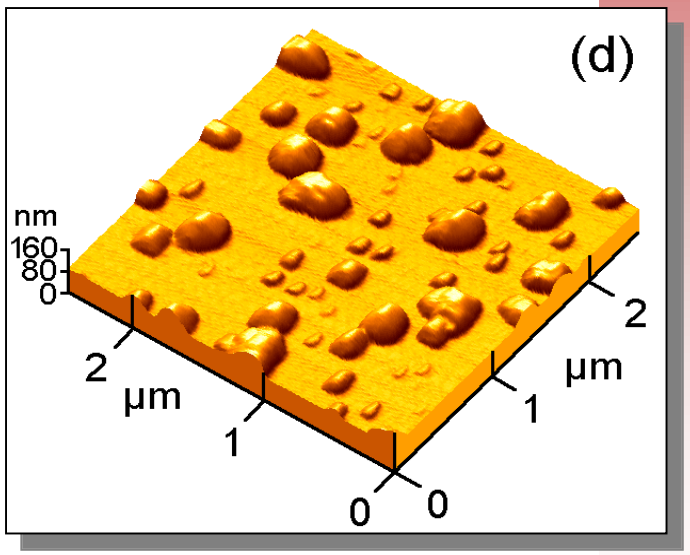

Energetics of island formation

- Competing energies:
  - strain
  - surface
  - dislocations

- Contributions from:

- wetting layer

- islands

Wetting layer WL+2D platelet WL+Strained island WL+Relaxed island

"Coverage"

AFM of Ge dots

- Analysis of aspect ratio provides measurement of relative amount of relaxed islands
- Ge/Si(001): Full range of relaxation examined

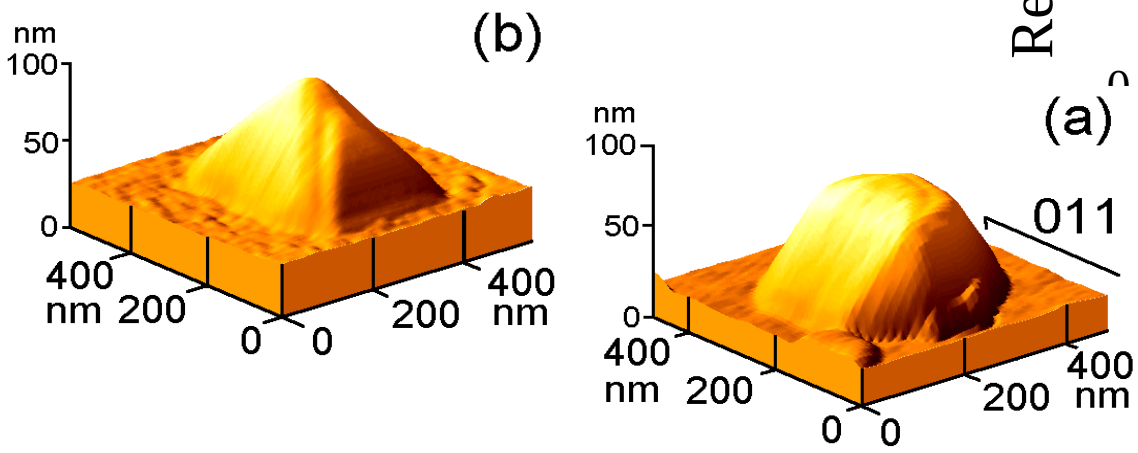

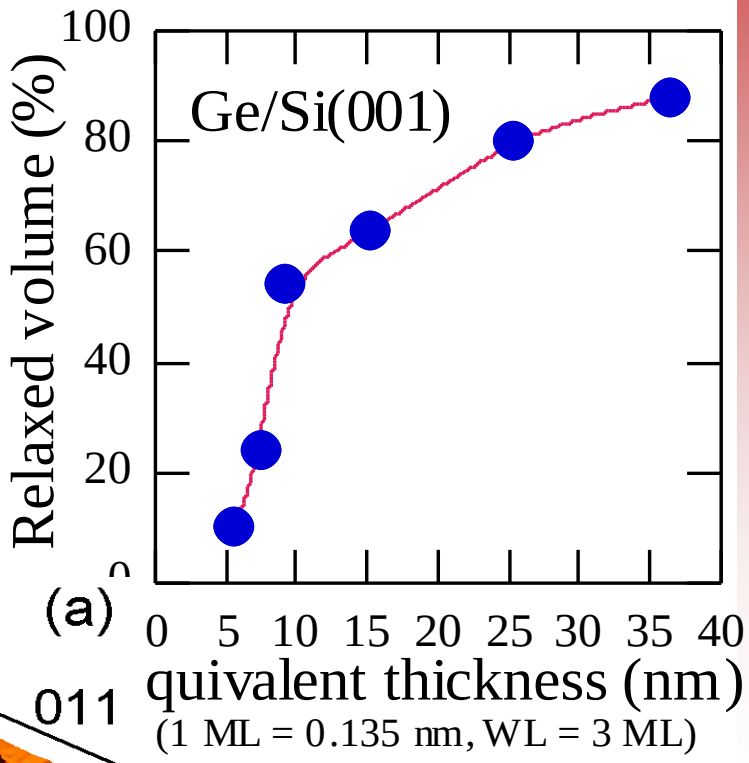

Quantum Dots: Ge edge XAFS

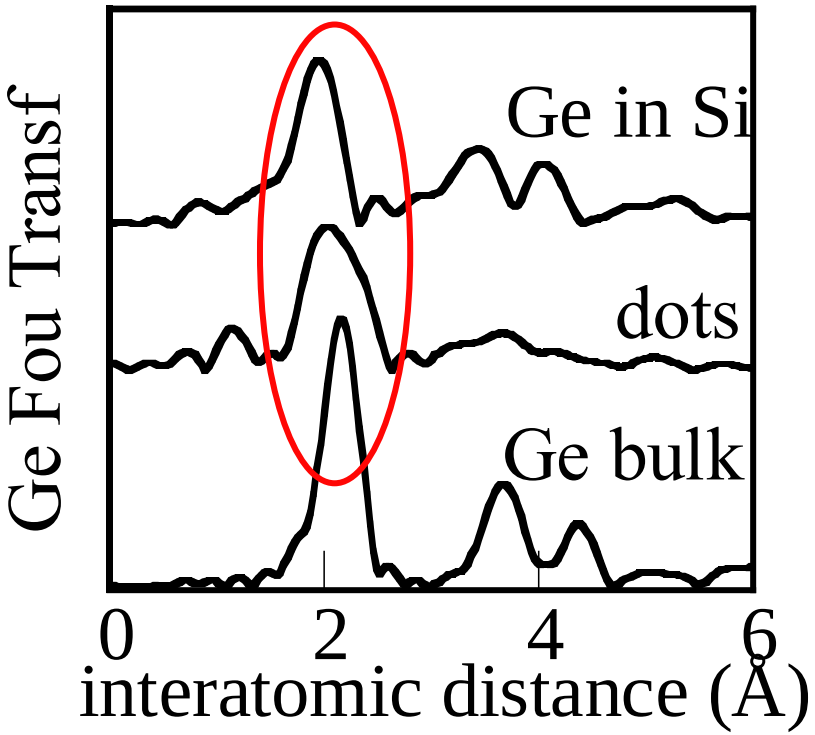

- Assuming random alloy average composition is $Ge_{0.70}Si_{0.30}$

Conventional SK growth

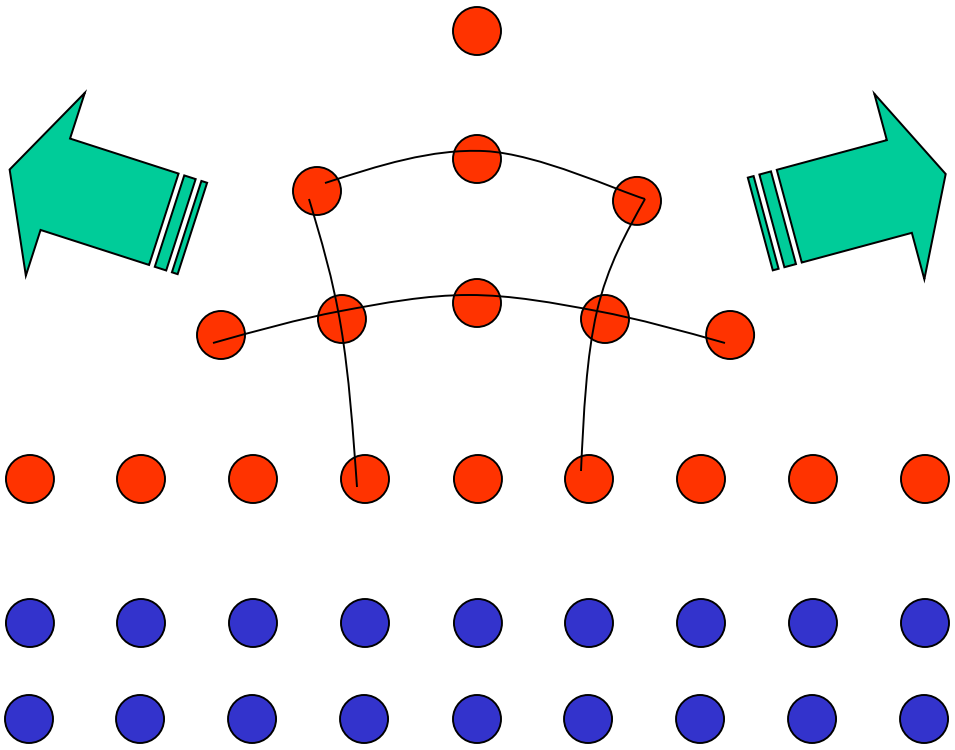

SK growth with interdiffusion

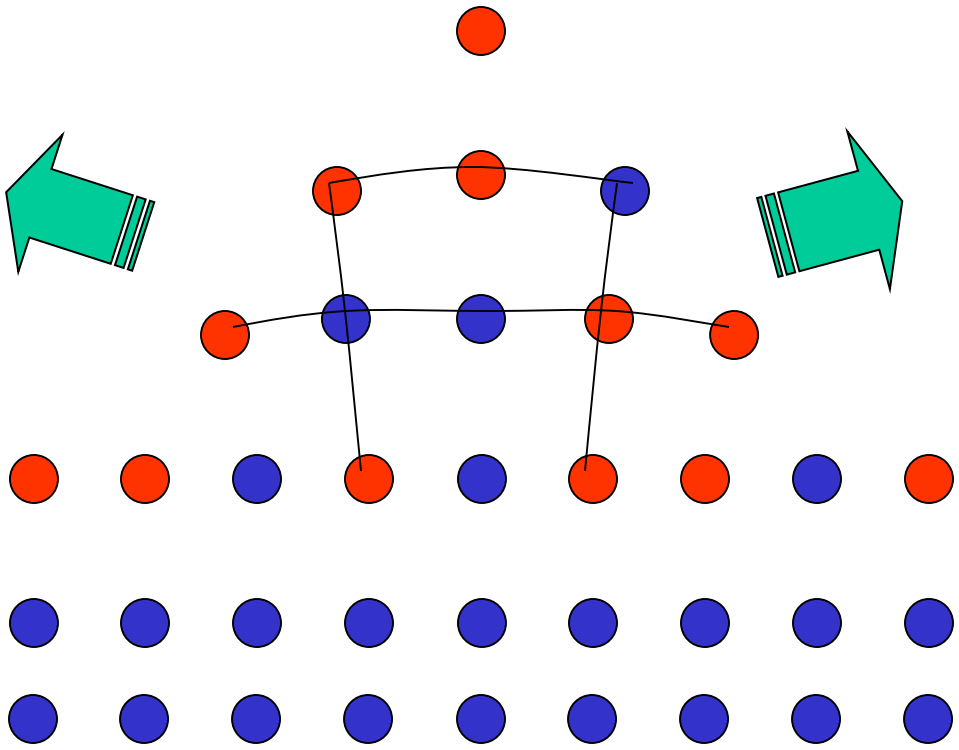

Metallic nanostructures

- One of the first applications of XAFS
- Exploits high resolution in first coordination shells

Clusters: bond length contraction

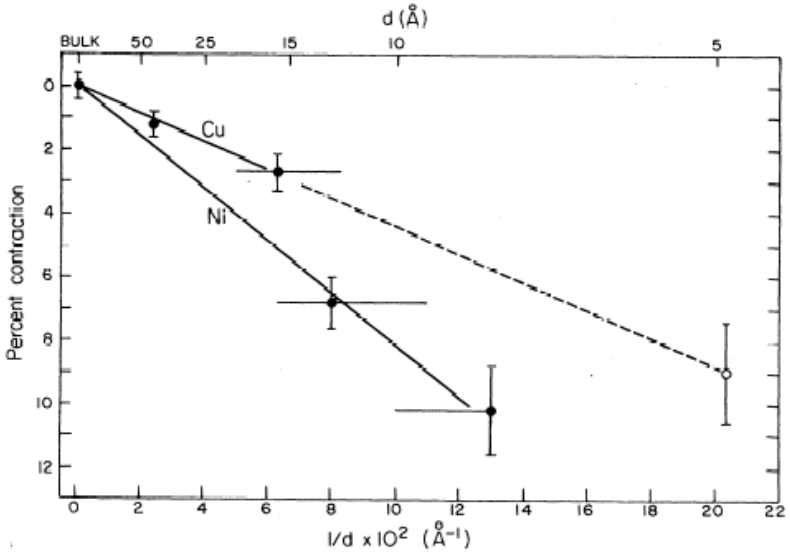

Apai et. al.,
Phys. Rev. Lett. **43**, 165 (1979)

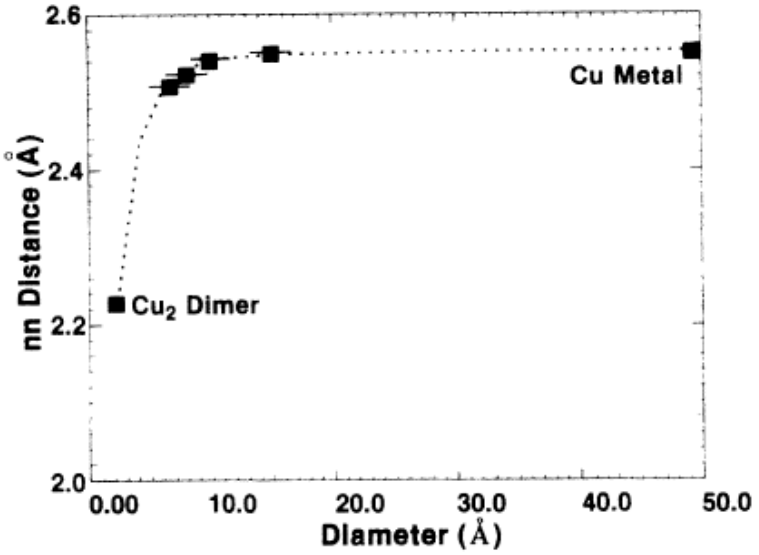

FIG. 4. Variation in interaction distance as a function of particle size.

Montano et. al.,
Phys. Rev. Lett. **56**, 2076 (1986)

- A bond length contraction has been found for weakly supported metallic clusters (Ni, Cu, Au……) for d < 100 Å

Bond length contraction

- A macroscopic surface tension interpretation ("liquid drop") can explain the bond length contraction
  - f surface tension,
    κ bulk modulus
    r radius of spherical particle
  - Montano et. al.
    Phys. Rev. B **30**, 672 (1984)
    Balerna et. al.,
    Phys. Rev. B **31** 5058 (1985)

$$\frac{\Delta R}{R} = -\frac{2}{3} f \frac{\kappa}{r}$$

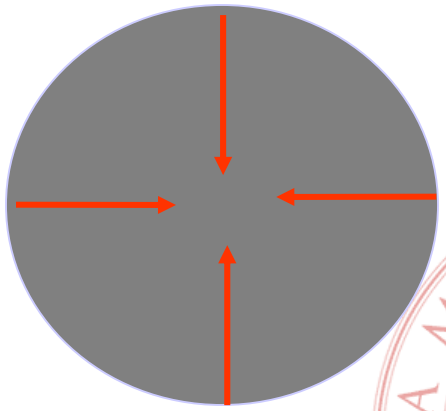

Dynamic properties of Au clusters

- In the harmonic approximation, the Mean-Square-Relative-Displacement, σ^2, damps the EXAFS signal with a term

$$e^{-2k^2\sigma^2}$$

$$\sigma_{0j}^2 = \left\langle \left| \left(\vec{u}_0 - \vec{u}_j\right) \bullet \hat{R}_{0j} \right|^2 \right\rangle$$

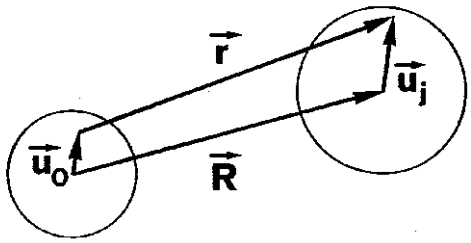

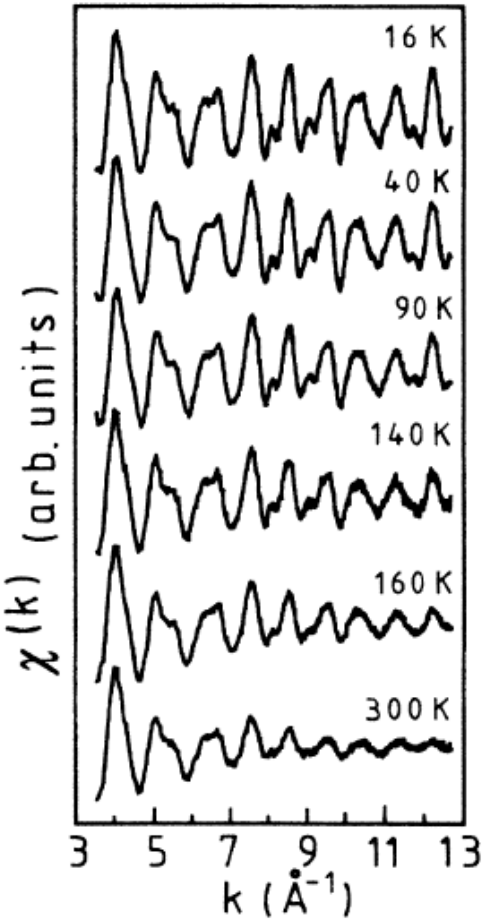

Bulk Au

Dynamic properties of Au clusters

- As the cluster dimensions decrease an enhacement of σ^2 is evident
- Surface atoms have less motion constraints
- High surface-to-volume ratio for nanoclusters
- Values reproduced by numerical model for free sphere phonon DOS which includes surface modes
- Balerna and Mobilio, Phys. Rev. B **34**, 2293 (1986)

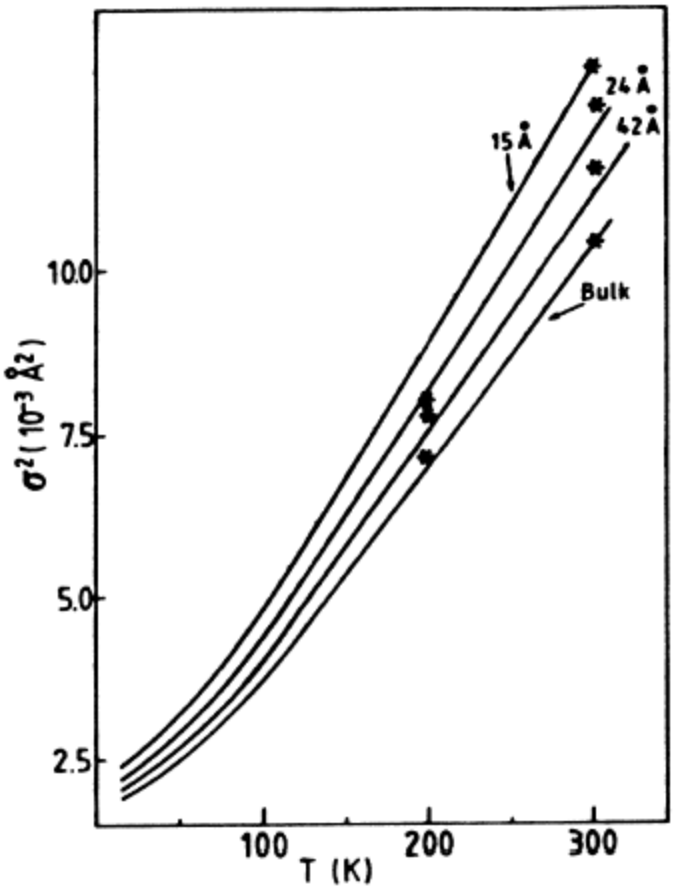

High resolution inelastic x-ray scattering at Ti K-edge to study light – induced plasmonic electron transfer processes in Au/TiO_2 nanocomposites

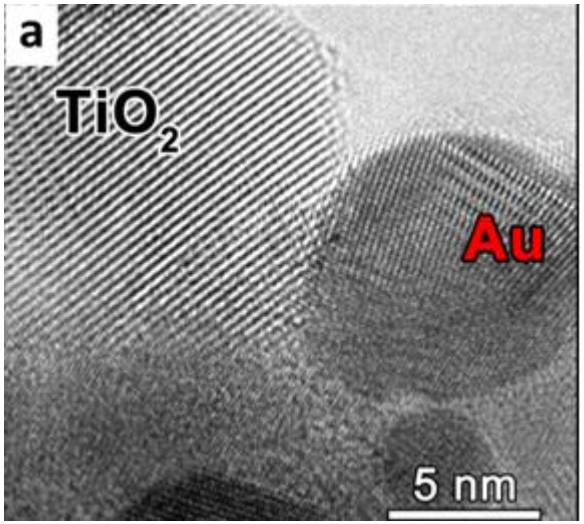

Amidani et al.,
Angew. Chem. Int. Ed. 54, 5413 (2015)

Motivation

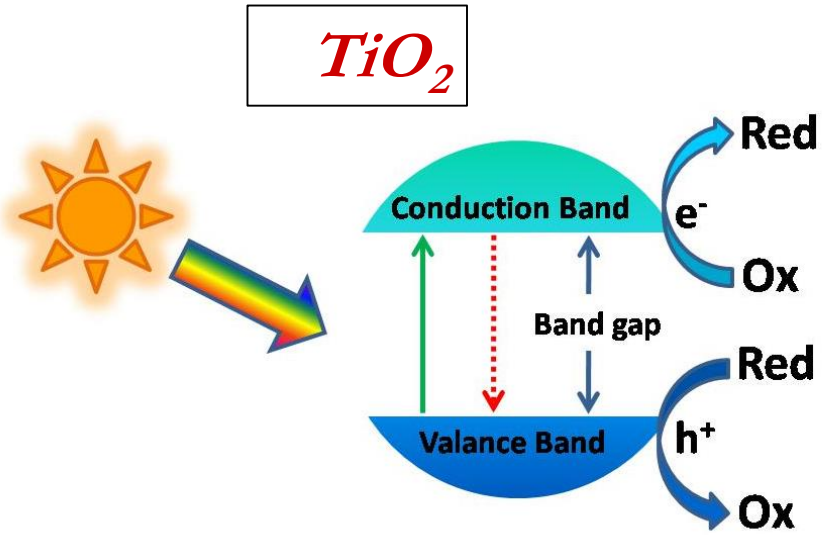

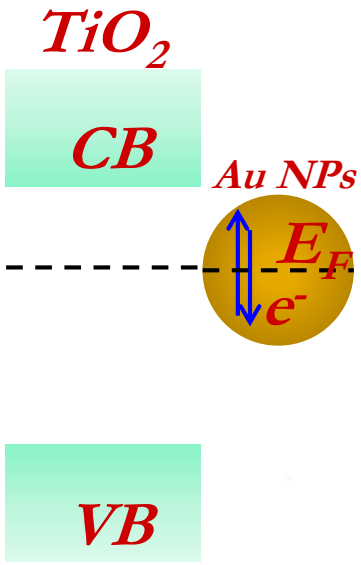

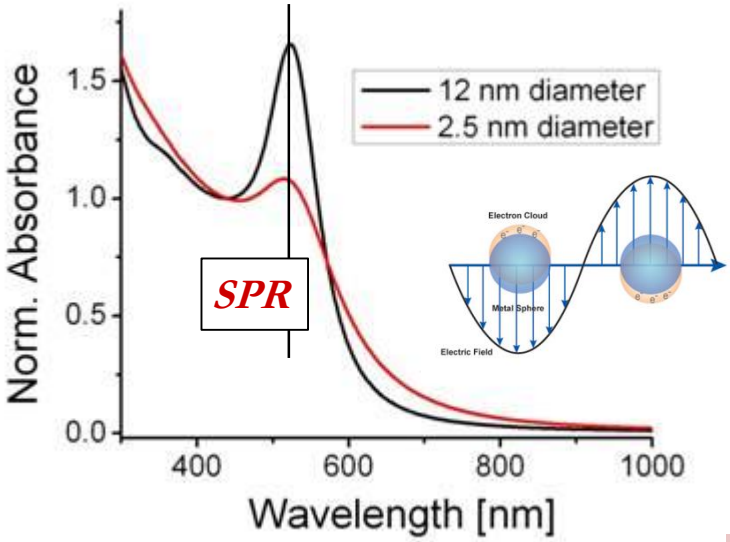

sensitize TiO_2 to visible light by coupling TiO_2 with metallic nanoparticles to exploit the surface plasmon resonace

RIXS @ ID26 ESRF

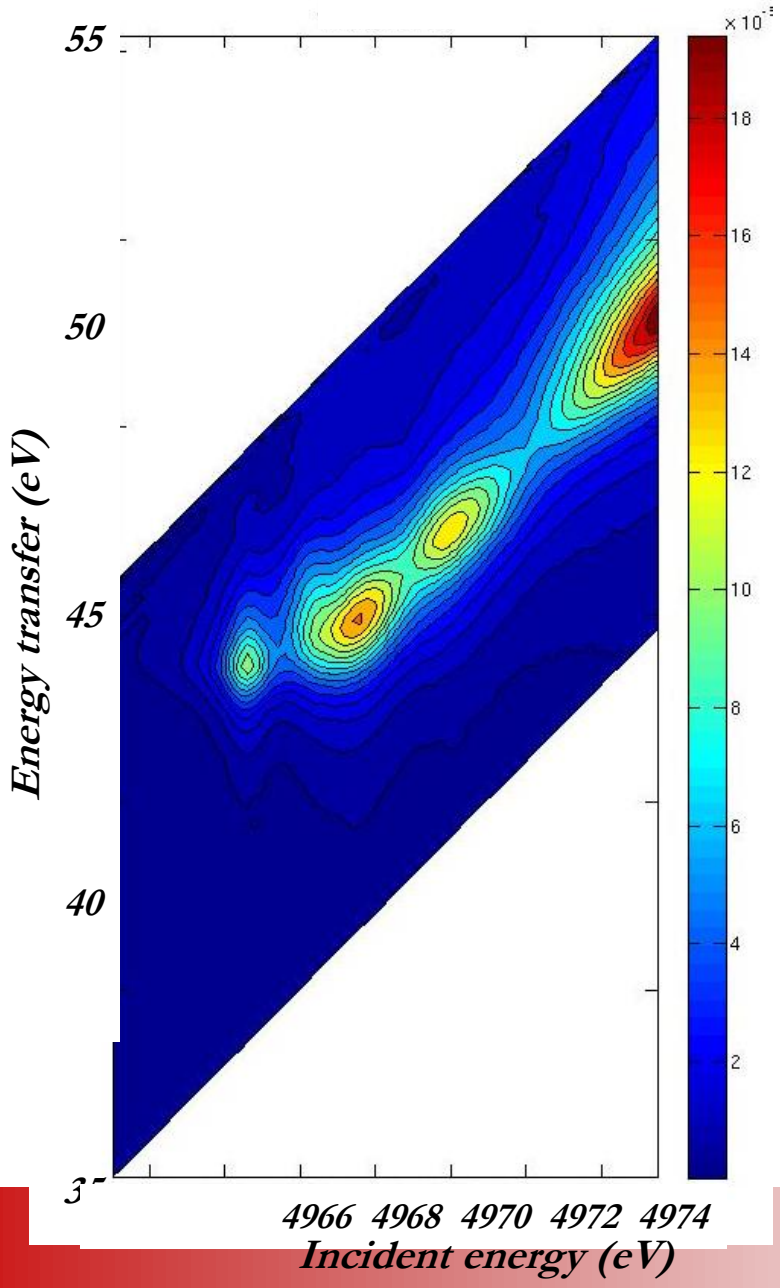

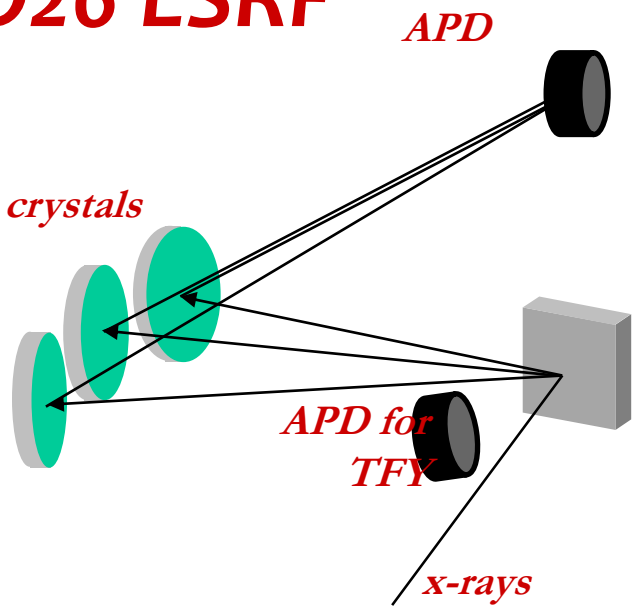

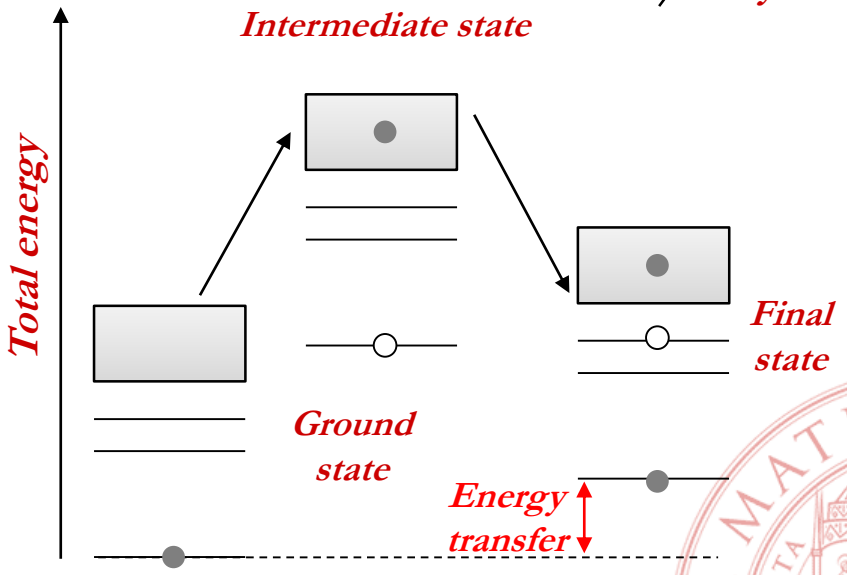

RIXS @ ID26 ESRF

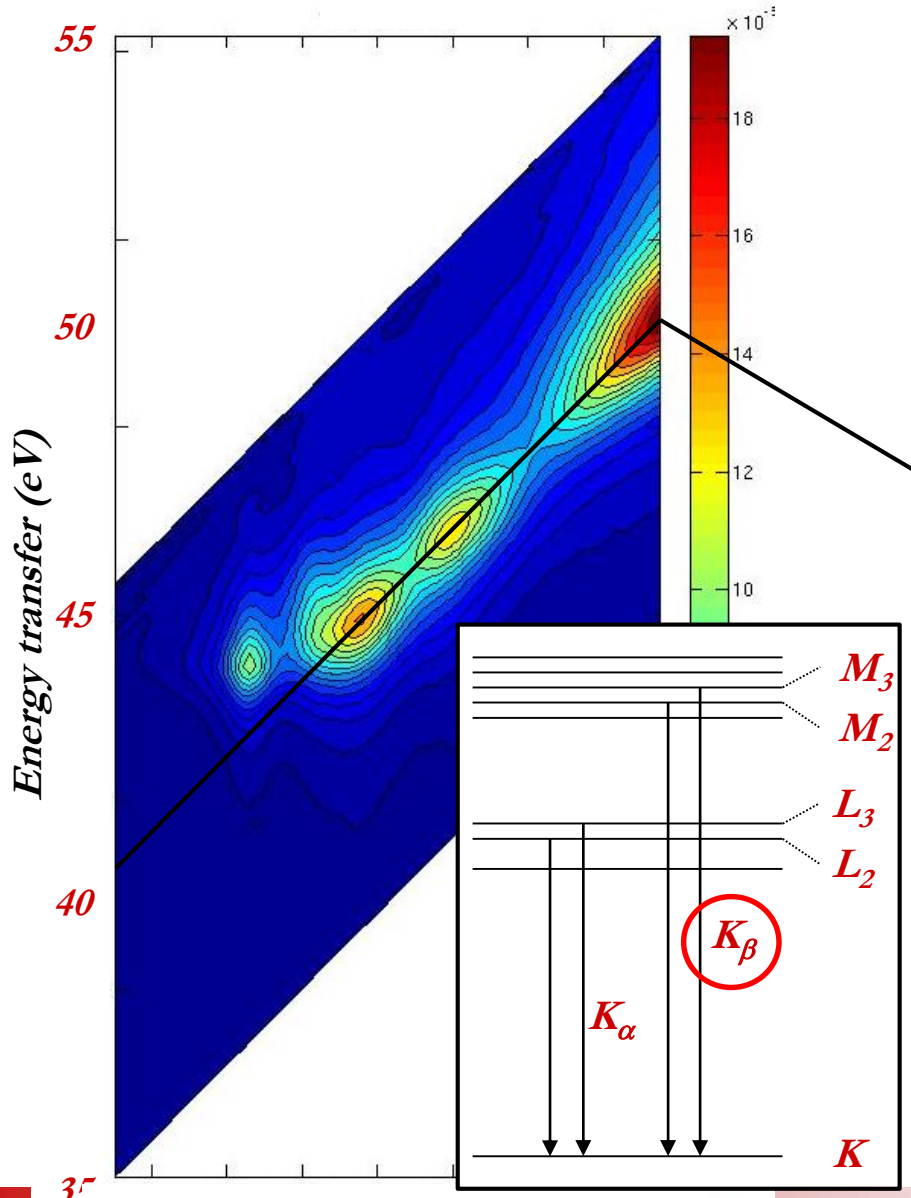

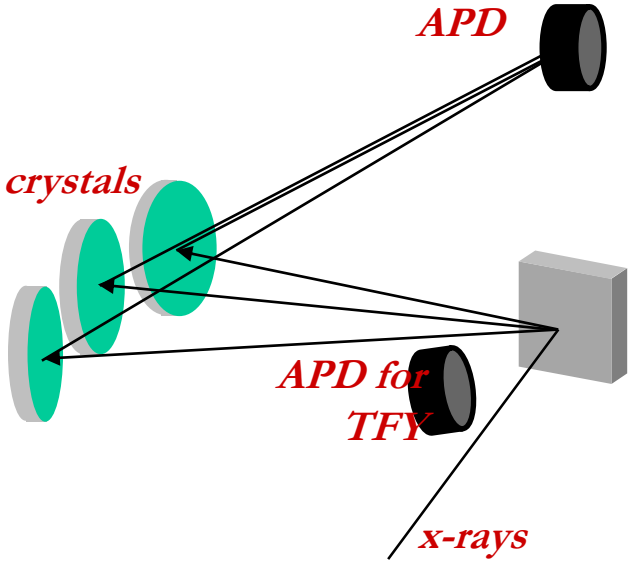

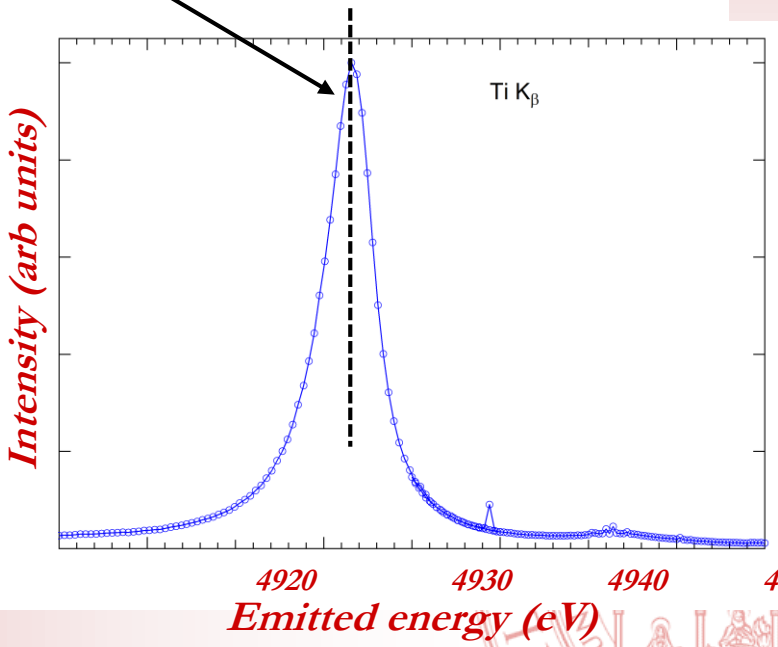

RIXS @ ID26 ESRF

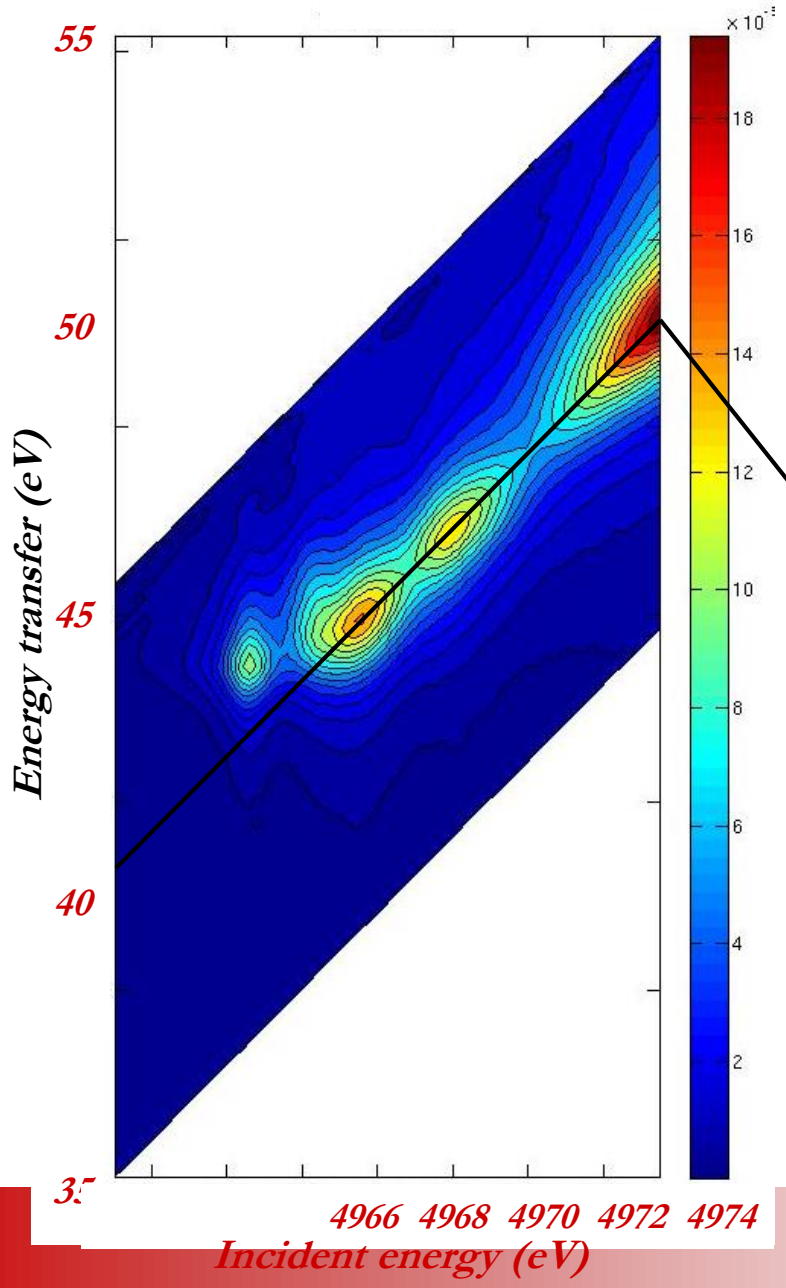

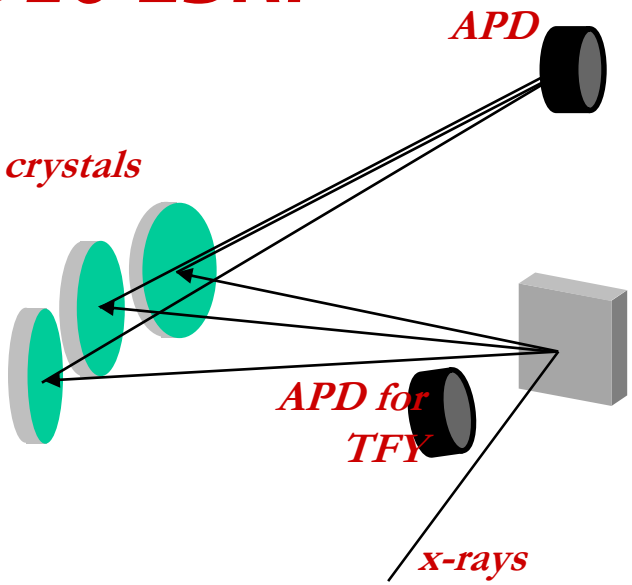

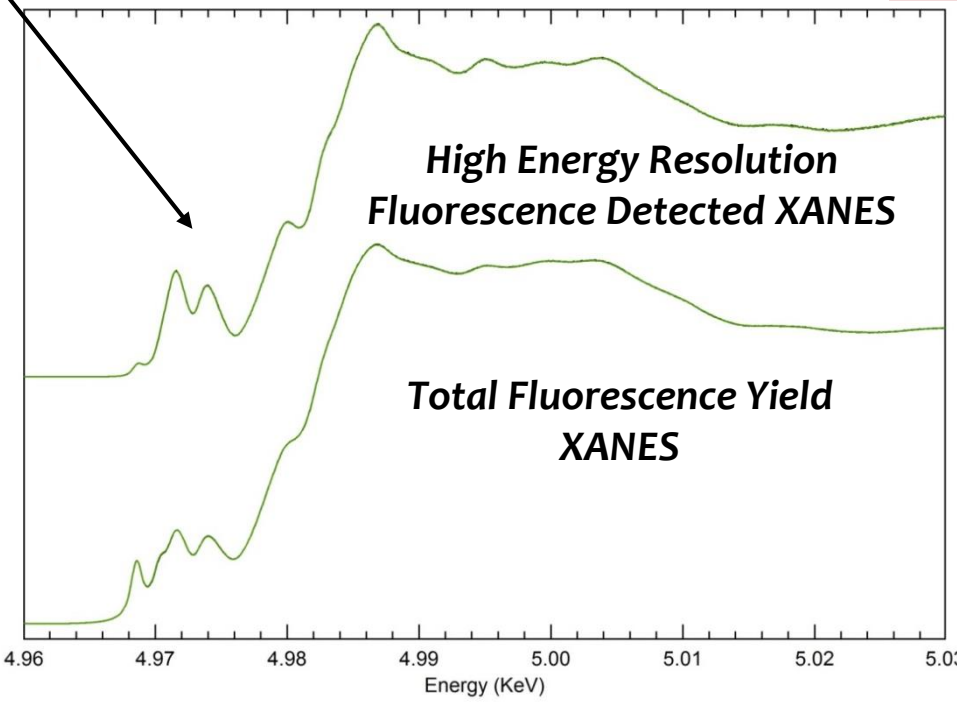

Differential spectra

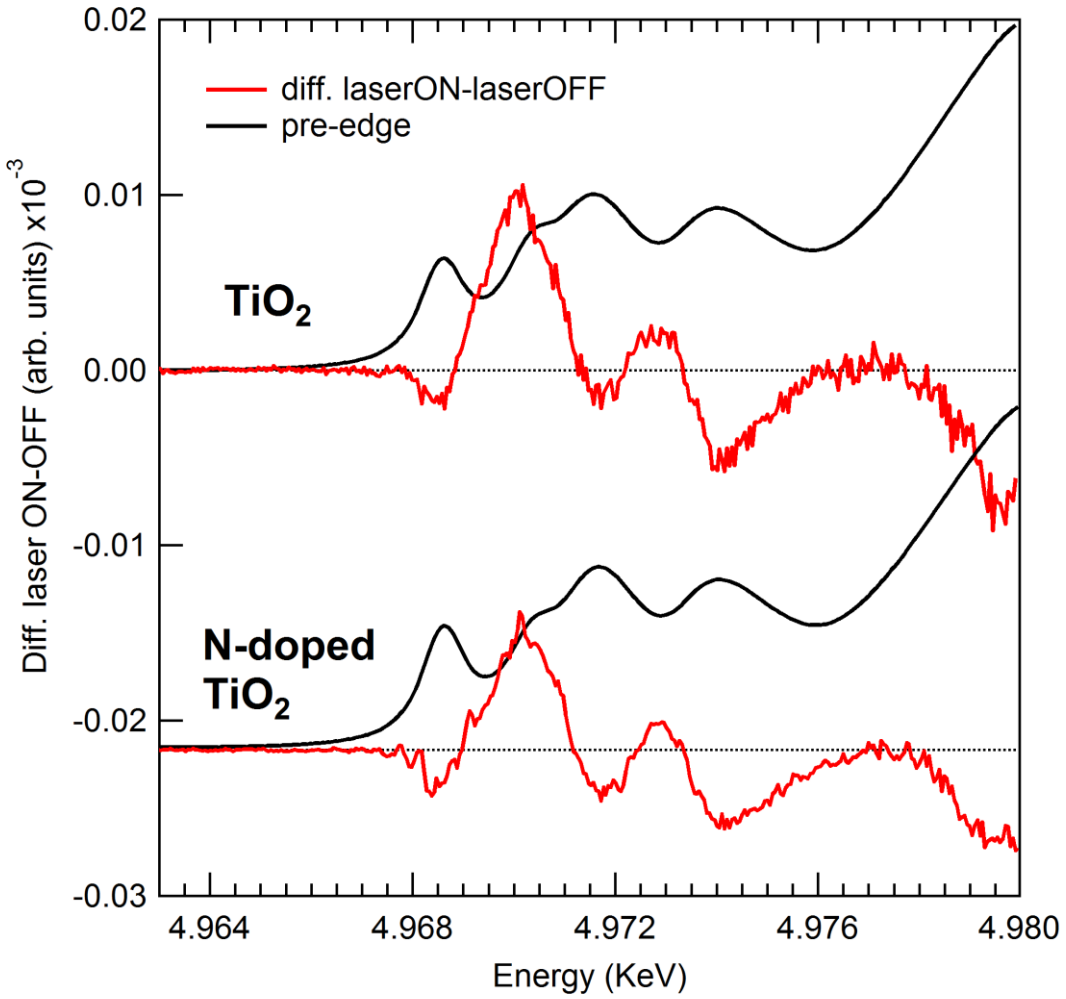

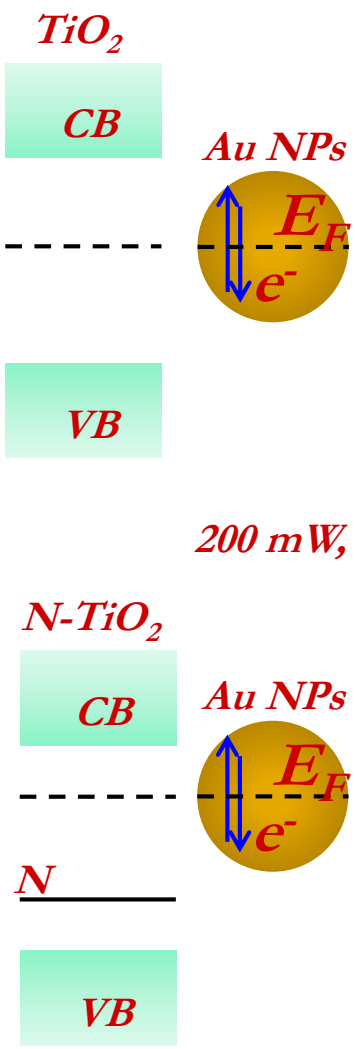

CW laser, 532 nm,

200 mW, 2 mm diameter spot

1. *Significant differences detected on samples with Au*
2. *No / small spectral differences on samples without Au*

Electron transfer from Au to TiO_2

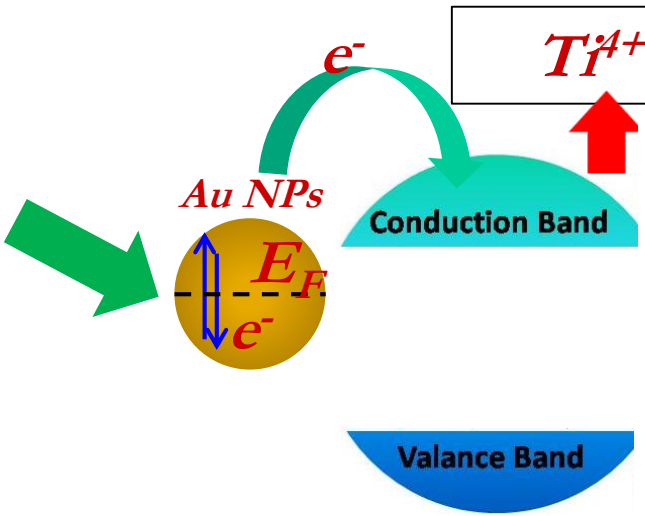

$$Ti^{4+} + e^- \rightarrow Ti^{3+}$$

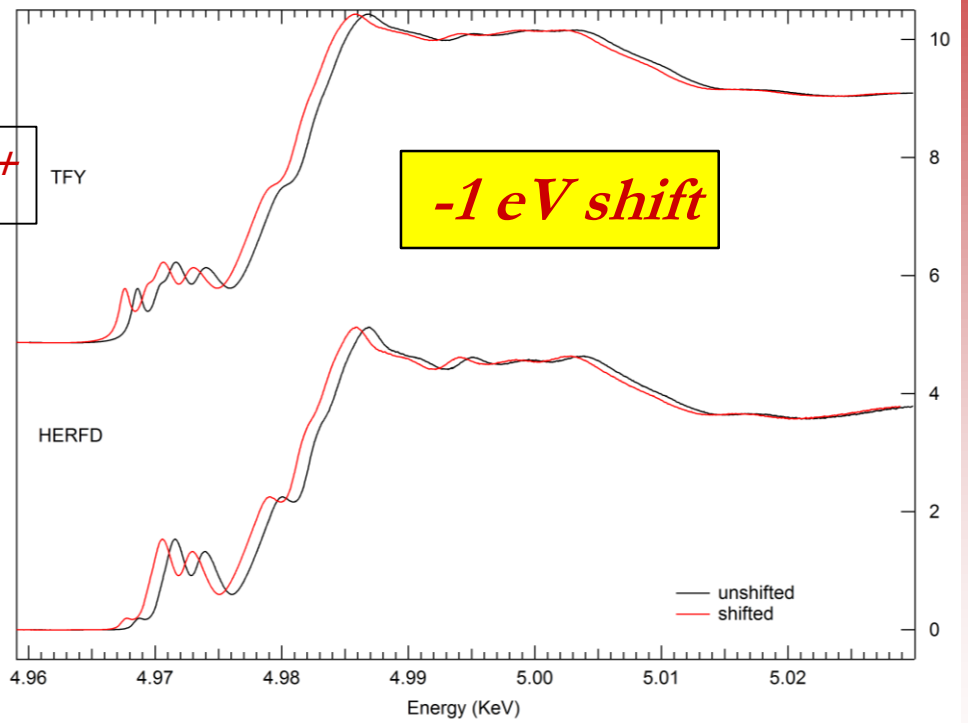

Electron transfer from Au to TiO_2

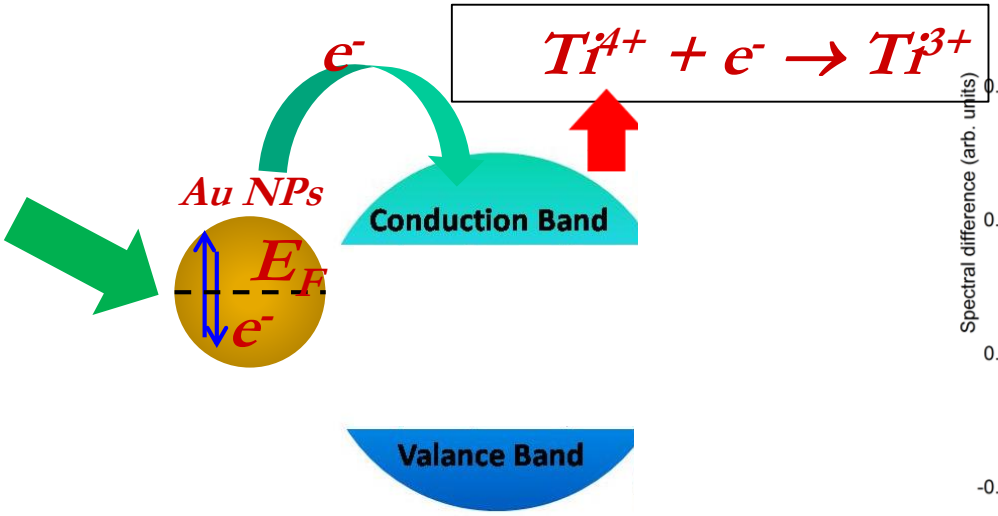

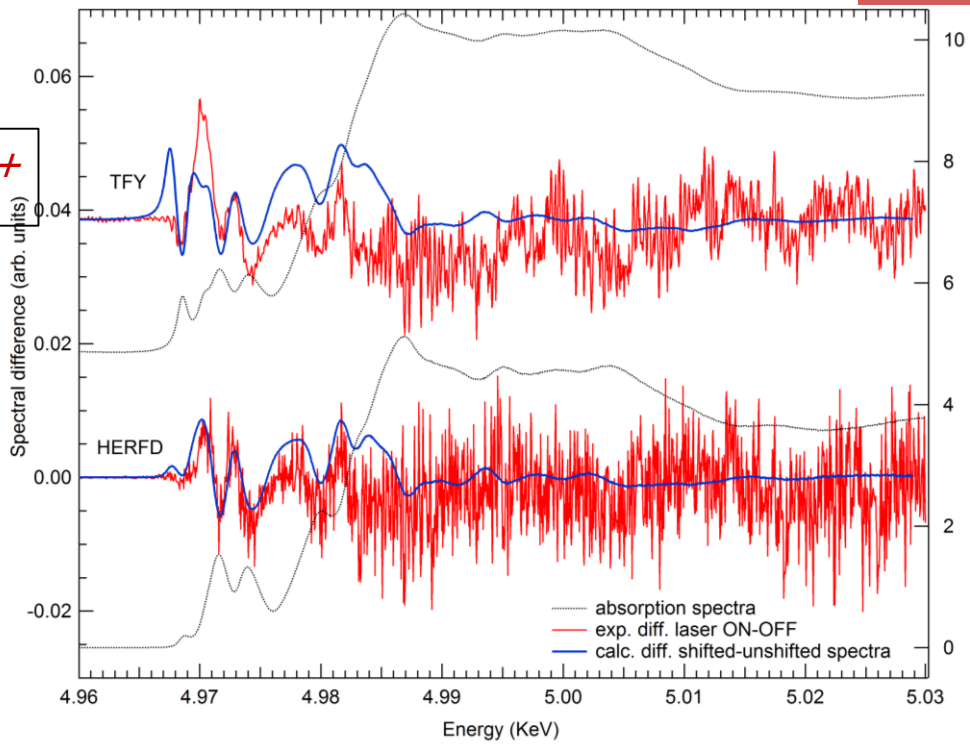

Evidence for hot electron transfer to Ti sites

More in depth…..

- Different «cuts» in the RIXS plane probe the effect of transitions to different final states
- HERFD-I
  - Mainly A3 and B: delocalized final states
- HERFD-II
  - Mainly A1 and A2: Localized final states

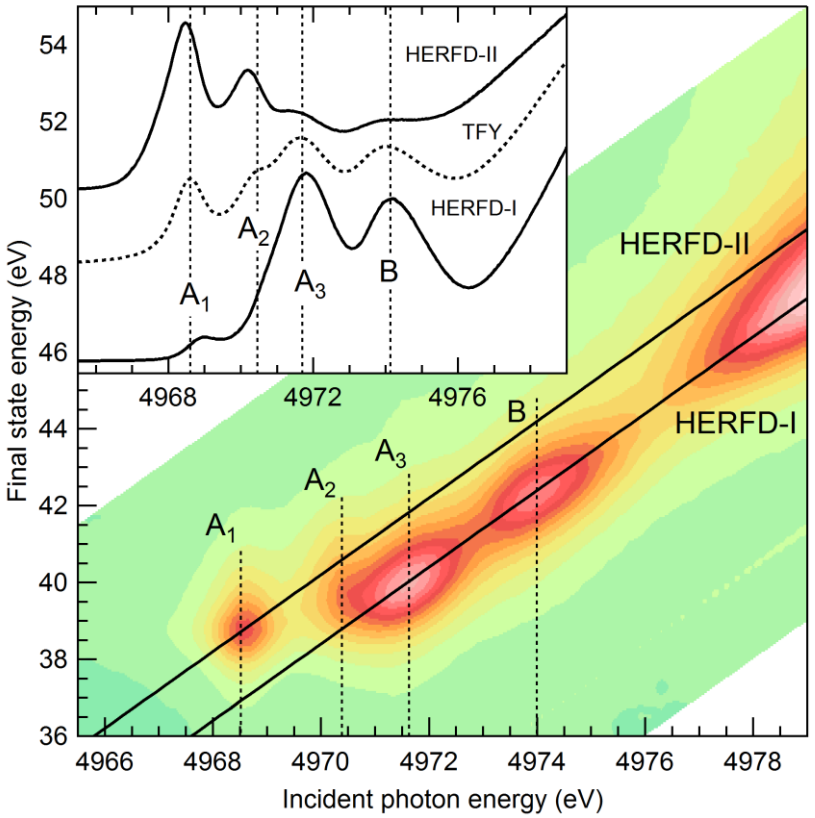

More in depth……

- HERFD-I differential spectra in excellent agreement with «shifted – unshifted»: charge transfer to delocalized states, without change in structure

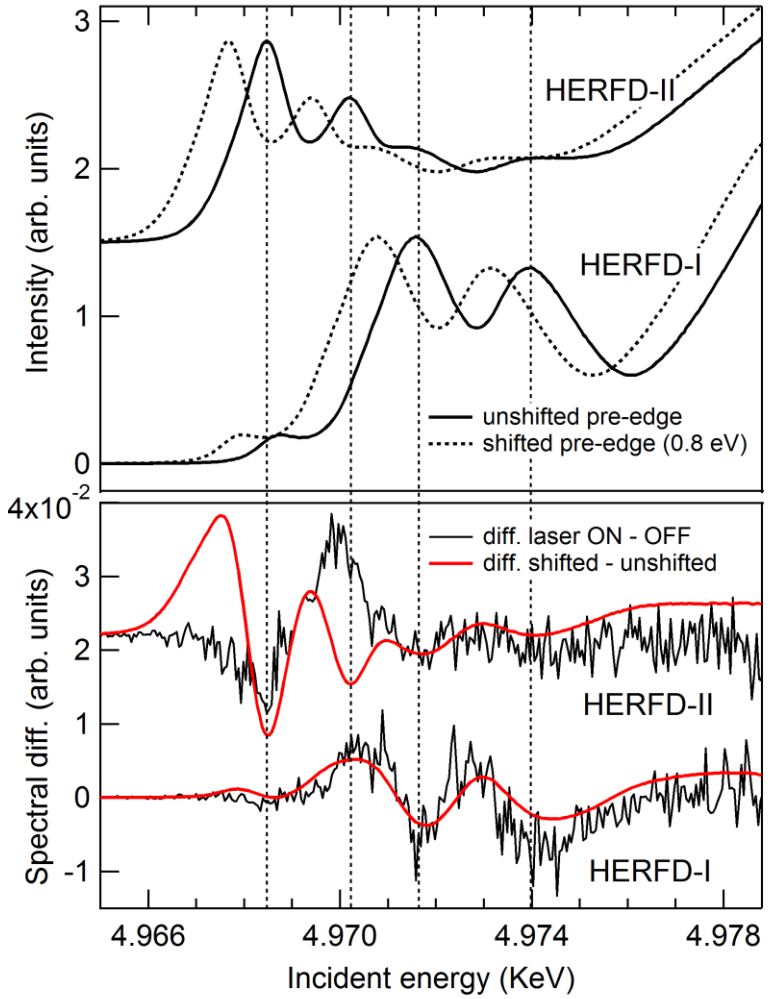

More in depth……

- HERFD-II differential spectra in not so good agreement with «shifted – unshifted»: charge transfer to localized states involves structural rearrangement

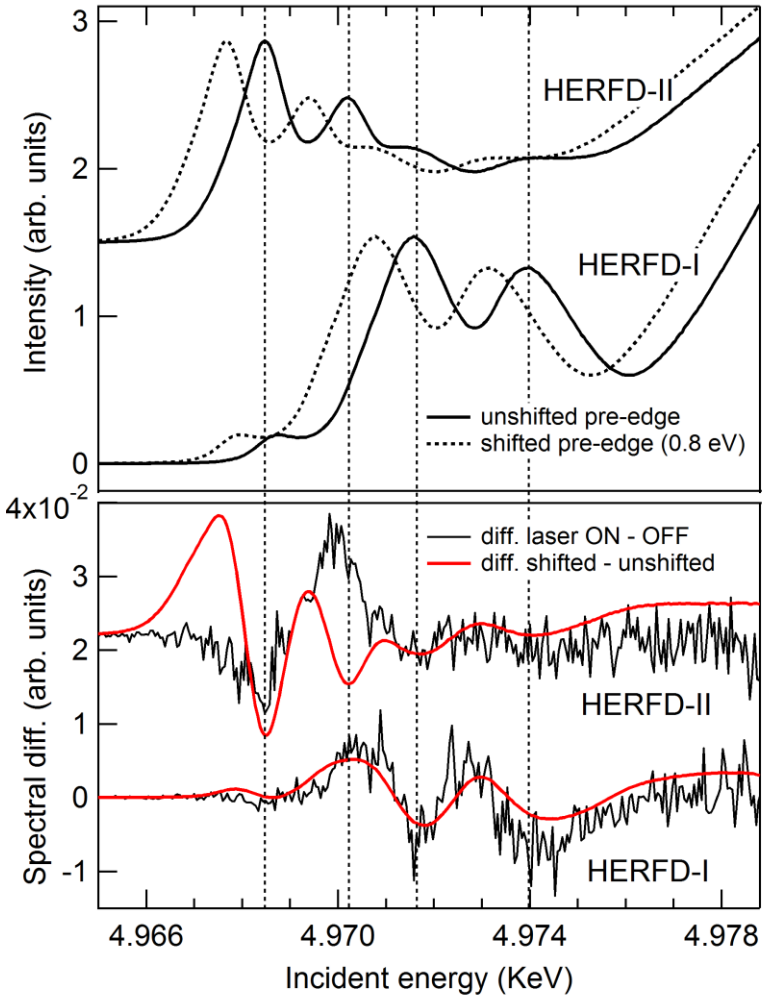

Conclusions on electron transfer in TiO2 NP

- Electron transfer processes from Au NP to TiO2 detected via differential HERFD XANES
- Different «cuts» in the RIXS plane can identify transitions to different final states
- Transitions to delocalized TiO2 states corresponds to simple charge trasfer with no structural rearrangement

Conclusions

- XAFS has been used to address important structural issues in materials/nano science
- It has specific advantages, especially
  - Atomic selectivity
  - Sensitivity to high dilutions & surfaces/interfaces
  - Equally applicable to ordered or disordered matter
  - EXAFS: high resolution for first few coordination shells
  - XANES:
    - valence/oxidation state
    - 3D structural sensitivity
  - μm spot size now available and decreasing fast
  - Time resolution in the 10 -100 ps range available and with FELs decreasing to 10 fs
  - Combined use of XAFS, XES & RIXS

Some useful review works by the author

- F. Boscherini, "XAFS in the study of semiconductor heterostructures and nanostructures" in Characterization of Semiconductor Heterostructures and Nanostructures, 2nd edition, edited by C. Lamberti and G. Agostini. ISBN 978-0-444-59551-5. DOI 10.1016/B978-0-444-59551-5.00007-8. Elsevier, 2013.
- F. Boscherini, "Dopants" in X-ray Absorption Spectroscopy of Semiconductors, edited by C.S. Schnor and M. Ridgway, Springer Series in Optical Sciences 190, 2015; ISBN-10: 3662443619 DOI 10.1007/978-3-662-44362-0_4. Springer, 2015.
- F. Boscherini, "Applications of XAFS to nanostructures and materials science", in Synchrotron Radiation: Basics, Methods and Applications, edited by F. Boscherini, C. Meneghini and S. Mobilio,. ISBN: 978-3-642-55314-1. DOI 10.1007/978-3-642-55315-8_17. Springer, 2015
- G. Ciatto and F. Boscherini, "Structure of nitrogen – hydrogen complexes from x-ray and synchrotron radiation techniques" in Hydrogenated dilute nitride semiconductors: theory, properties and applications, edited by G. Ciatto, Pan Stanford Publishing, 2015. ISBN 978-981-4463-45-4
- F. Boscherini, "Semiconductors", in X-Ray Absorption and X-Ray Emission Spectroscopy: Theory and Applications, First Edition. Edited by J. A. van Bokhoven and C. Lamberti. Published 2015 by John Wiley & Sons.

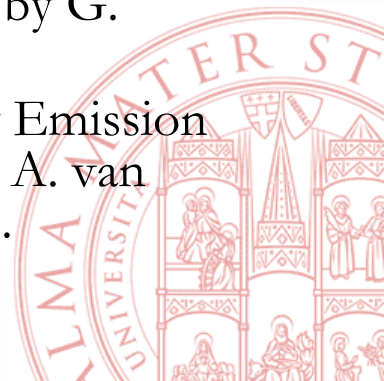

Bologna


TRENTO
UDINE
AOSTA
TRIESTE
MILANO
VENEZIA
TORINO
GENOVA
BOLOGNA
FIRENZE
PESCARA
L'AQUILA
ROMA
BARI
NAPOLI
TARANTO
© IANN SpA 2002 - © Tele Atlas digital mapping

What is Bologna famous for?

- University: Alma Mater Studiorum –1088 AD

Guglielmo Marconi (1874 – 1937): radio

Luigi Galvani (1737 – 1798) bioelectricity

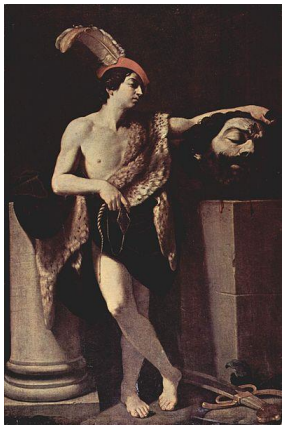

Guido Reni (1575 – 1642) painter

Lamborghini cars

Ducati motorbikes

Mortadella

Tagliatelle al ragù